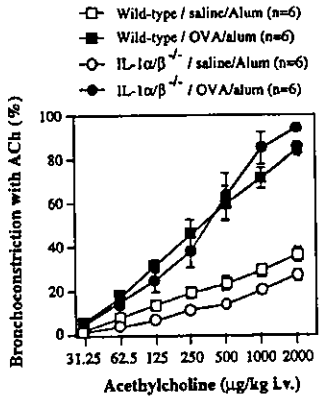

Fig. 1. AHR to ACh in IL-1α/β$^{-/-}$ mice sensitized with OVA/alum. AHR was induced to ACh in IL-1α/β$^{-/-}$ mice sensitized with alum alone (open symbols) or OVA/alum (closed symbols). Squares, wild-type mice; circles, IL-1α/β$^{-/-}$ mice. Data indicate the average of each mouse group ± SEM.

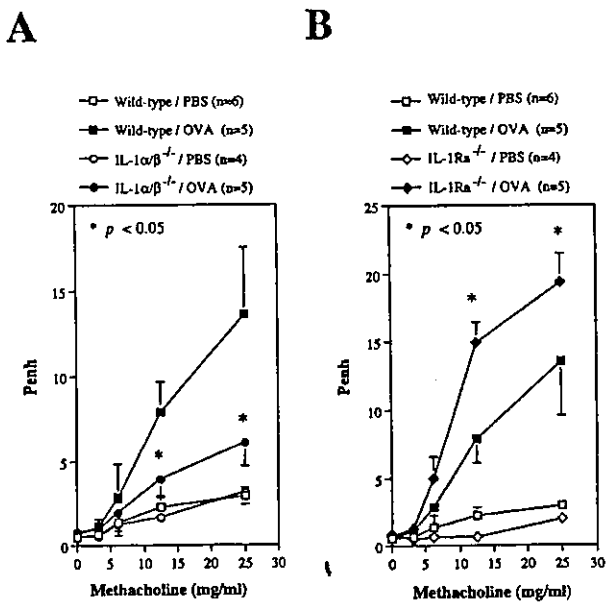

Fig. 2. AHR to methacholine in IL-1α/β$^{-/-}$ and IL-1Ra$^{-/-}$ mice sensitized with OVA/PBS without alum. AHR was induced to methacholine in IL-1α/β$^{-/-}$ and IL-1Ra$^{-/-}$ mice sensitized with PBS alone (open symbols) or OVA/PBS (closed symbols). (A) Wild-type (squares) and IL-1α/β$^{-/-}$ (circles) mice. (B) Wild-type (squares) and IL-1Ra$^{-/-}$ (diamonds) mice. Data indicate the average of each mouse group ± SD. These results were reproduced in three independent experiments. *$P < 0.01$ versus wild-type mice.

Results

Involvement of IL-1 in AHR

Although eosinophil infiltration into the lungs decreases in IL-1RI$^{-/-}$ mice on a 129 × B6 background (14), the involvement of IL-1 in the development of AHR remained to be studied. Thus, to determine whether IL-1 is necessary for the induction of AHR, we examined the role of IL-1 in this response using IL-1α/β$^{-/-}$ mice on a BALB/cA background following sensitization to OVA. First, we examined AHR induced by OVA/alum. Upon sensitization with OVA/alum, AHR in response to methacholine stimulation was not different between wild-type and IL-1α/β$^{-/-}$ mice (Fig. 1). Moreover, mutant mice immunized with OVA/alum exhibited a similar level of eosinophil infiltration into the lungs and similar IgE levels in sera as wild-type mice (data not shown).

Since we previously experienced that the function of IL-1 in the humoral immune response was substituted by other cytokines in the presence of adjuvant (18), we next examined AHR induced by OVA in the absence of alum. Twenty-four hours after the final OVA inhalation, AHR to methacholine in IL-1α/β$^{-/-}$ mice was significantly reduced compared with that observed in wild-type mice (Fig. 2). Consistent with the reduced AHR in IL-1α/β$^{-/-}$ mice, the number of lung-infiltrating cells in IL-1α/β$^{-/-}$ mice as revealed by the histology following OVA inhalation was less than that seen for wild-type mice (data not shown). The total cell numbers in the bronchoalveolar lavage of IL-1α/β$^{-/-}$ mice were decreased compared with that in wild-type mice (data not shown).

On the other hand, AHR to methacholine in IL-1Ra$^{-/-}$ mice was markedly increased compared with the response seen in wild-type mice (Fig. 2B). As expected, the inflammatory responses observed in IL-1Ra$^{-/-}$ mice given OVA were enhanced (data not shown). These results suggest that IL-1 functions in the development of AHR.

Roles of IL-1 in T_h2 cell activation during AHR

Although IL-1 is thought to promote both T_h1 and T_h2 cell-mediated immune responses, the role of IL-1 in T_h2 cell activation during AHR remains poorly understood (15–20). Therefore, we assessed allergen-specific T cell responses in IL-1α/β$^{-/-}$ mice challenged with OVA. The OVA-specific T cell proliferative responses of IL-1α/β$^{-/-}$ mice were profoundly decreased in comparison with those in wild-type mice (Fig. 3A). The levels of the T_h2 cytokines IL-4 and IL-5 were also reduced in the supernatants of the IL-1α/β$^{-/-}$ LN cell cultures (Fig. 3B). In contrast, OVA-specific proliferative responses and the production of IL-4 and IL-5 in LN cells increased in IL-1Ra$^{-/-}$ mice (Fig. 3C and D). These results suggest that IL-1 plays an important role in T_h2 cell activation during AHR.

Allergen-specific IgG1 and IgE production

The levels of OVA-specific IgG1 and IgE in sera were determined by ELISA to assess if reduced T_h2 cell activation affected B cell antibody production in IL-1α/β$^{-/-}$ mice. OVA-specific IgG1 and IgE levels in sera obtained from IL-1α/β$^{-/-}$ mice were significantly lower than those seen in wild-type mice (Fig. 4A). Sera from IL-1Ra$^{-/-}$ mice, however, contained elevated levels of IgG1 and IgE as compared to those from wild-type mice (Fig. 4B), suggesting that IL-1 is necessary for T_h2 cytokine-dependent antibody production in AHR.

Roles of IL-1α and IL-1β in AHR

To determine whether IL-1α or IL-1β, or both, are involved in the development of AHR, we sensitized IL-1α$^{-/-}$ and IL-1β$^{-/-}$ mice with OVA in the absence of adjuvant. The AHR induced

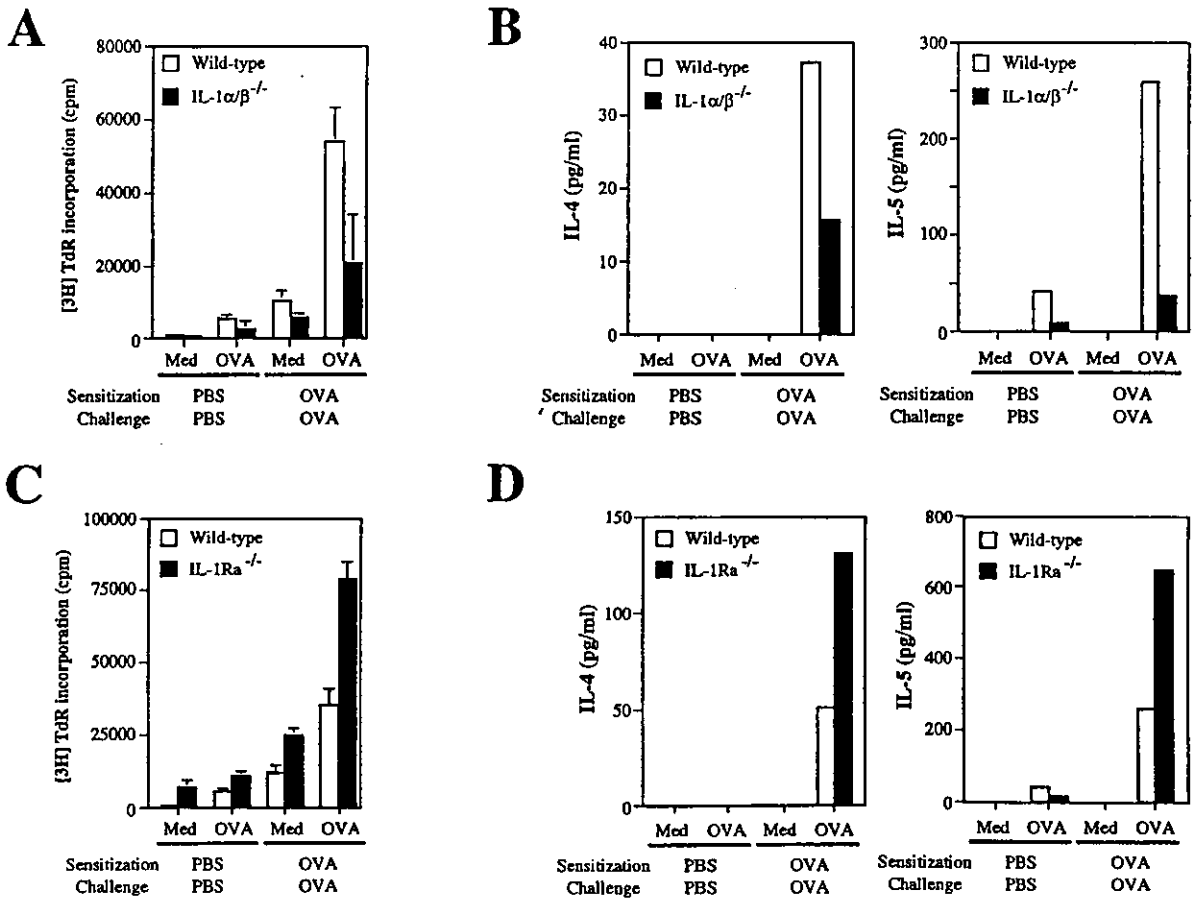

Fig. 3. OVA-specific T cell responses in IL-1α/β$^{-/-}$ and IL-1Ra$^{-/-}$ mice during AHR. The proliferative responses of LN cells derived from OVA-challenged wild-type, IL-1α/β$^{-/-}$ and IL-1Ra$^{-/-}$ mice were measured by [^{3}H]thymidine uptake. Twenty-four hours after the final OVA inhalation, submaxillary LN cells were cultured in the absence or presence of 40 μg/ml OVA for 72 h. The averages ± SD of triplicate experiments are shown. These results were reproduced in three independent experiments. IL-4 and IL-5 levels in the pooled supernatant of three wells from the proliferative response assay were determined by ELISA. These results were reproduced in three independent experiments. (A) OVA-specific proliferative responses, (B) IL-4 and IL-5 levels in wild-type and IL-1α/β$^{-/-}$mice, (C) OVA-specific proliferative responses, and (D) IL-4 and IL-5 levels in wild-type and IL-1Ra$^{-/-}$mice.

to methacholine in IL-1α$^{-/-}$ mice was significantly reduced compared with that of wild-type mice (Fig. 5). Such responses in IL-1β$^{-/-}$ mice were also reduced in a similar fashion to IL-1α$^{-/-}$ mice (Fig. 5). These results suggest that both IL-1α and IL-1β are required for AHR development.

We next examined primary OVA-specific T cell responses, and found that the levels of proliferation of DO11.10 Tg T cells cultured with the antigen-presenting cells (APC) derived from IL-1α$^{-/-}$ and IL-1β$^{-/-}$ mice were partially, but not completely, decreased in the presence of OVA peptide in comparison to the wild-type levels (Fig. 6). The levels of OVA-specific IgE, but not IgG1, present in the sera of IL-1α$^{-/-}$ mice were significantly reduced compared with wild-type sera (Fig. 7). The production of both IgG1 and IgE in response to OVA in IL-1β$^{-/-}$ mice, however, was lower than that of wild-type mice. Similar observations were noted for the total Ig levels in the sera of non-immunized mice (Fig. 8). These results suggest that IL-1α and IL-1β have mutually complementary activities in T cell activation, but have differing effects on antibody production.

Discussion

In this study, we demonstrate that AHR is markedly reduced in IL-1α/β$^{-/-}$ mice, but exacerbated in IL-1Ra$^{-/-}$ mice, and that both IL-1α and IL-1β are required for this reaction. It was reported that the recruitment of eosinophils into the lungs was markedly reduced in IL-1RI$^{-/-}$ mice on a 129 × B6 F_1 background following OVA/alum sensitization (14). The magnitude of AHR and the number of lung-infiltrating eosinophils, however, were normal in IL-1α/β$^{-/-}$ mice on the BALB/cA background using a similar experimental protocol (Fig. 1 and data not shown). Then, in this study, we examined AHR in IL-1α/β$^{-/-}$ mice on a BALB/cA background using repeated OVA/PBS sensitization without alum. As alum induces excess

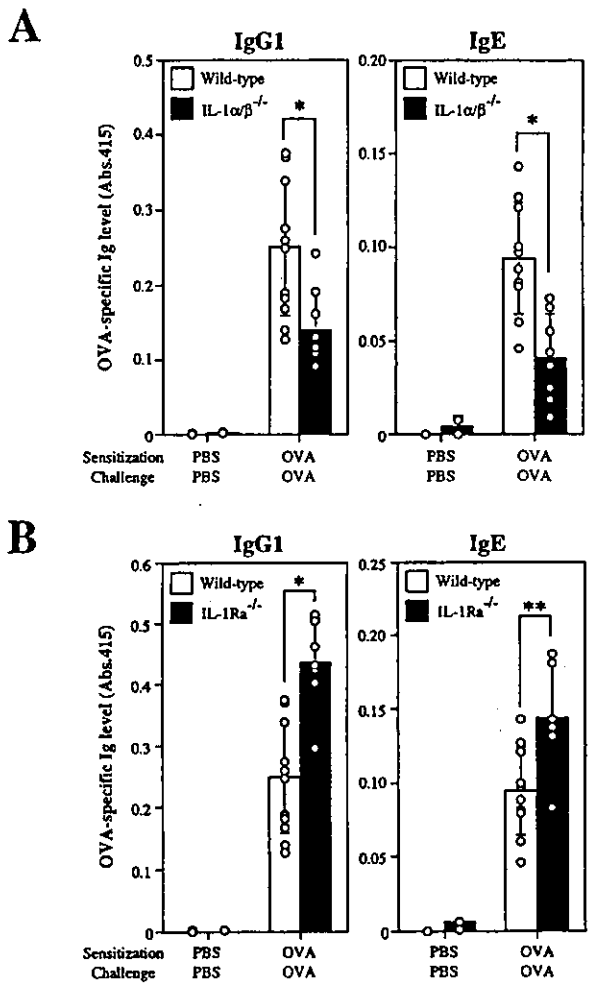

Fig. 4. OVA-specific IgG1 and IgE levels in sera from IL-1α/β$^{-/-}$ and IL-1Ra$^{-/-}$ mice during AHR. Sera were collected 24 h after the final inhalation. OVA-specific Ig levels were determined by ELISA. Each circle represents an individual mouse. The average and SD are shown. (A) Wild-type (n = 11) and IL-1α/β$^{-/-}$ (n = 8) mice. (B) Wild-type (n = 11) and IL-1Ra$^{-/-}$ (n = 7) mice. *P < 0.005 and **P < 0.01 versus wild-type mice.

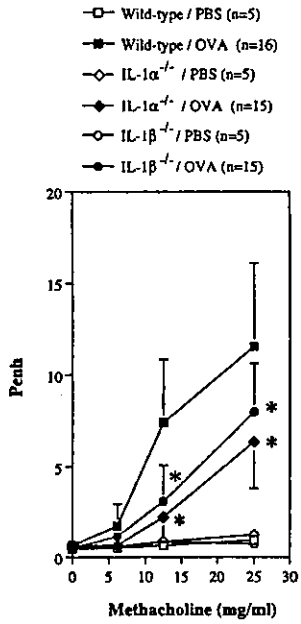

Fig. 5. AHR to methacholine in IL-1α$^{-/-}$ and IL-1β$^{-/-}$ mice sensitized with OVA without alum. AHR was induced to methacholine in wild-type (squares), IL-1α$^{-/-}$ (diamonds) and IL-1β$^{-/-}$ (circles) mice sensitized with either PBS alone (open symbols) or OVA/PBS (closed symbols). Data from two independent experiments are pooled and the averages of each mouse group ± SD are shown. *P < 0.01 versus wild-type mice.

T_h2 responses even in the absence of IL-4Rα signaling (27), the presence of alum may account for the differences obtained through the use of either OVA/alum or OVA/PBS. Since many asthmatic patients develop dramatic pathophysiological responses to low-dose allergen challenge (28), AHR induced by a weak inducer OVA/PBS, not OVA/alum, appears to reflect the general pathological predisposition of an individual. This notion is supported by the observation that both B cell-deficient and mast cell-deficient mice exhibit normal AHR development when sensitized with OVA/alum (29,30). This directly conflicts with the generally accepted notion that the activation of mast cells via antigen-IgE complexes is crucial for the development of AHR (31). In contrast, AHR in mast cell-deficient mice sensitized to OVA without alum was markedly reduced (24).

IL-1 functions as both a T cell activator and a pro-inflammatory cytokine. IL-1–IL-1RI signaling is responsible for the induction of VCAM-1 expression, recruiting eosinophils to the lungs during AHR (14). On the other hand, we showed that antigen-specific T cell proliferative responses, IL-4 and IL-5 production by T cells, and antigen-specific IgG1 and IgE secretion by B cells were reduced in IL-1α/β$^{-/-}$ mice during AHR, whereas these responses increased in IL-1Ra$^{-/-}$ mice compared with wild-type mice. These results suggest that IL-1 plays an important role in activating T_h2 cells. Consistently with these observations, involvement of IL-1 in T_h2 activation, that is either dependent or independent of IL-4 and requires Lck activation, has been suggested (15,17,18). Furthermore, IL-1 induces OX40 (CD134) expression on CD4$^+$ T cells (26), that plays an important role in T_h2 cell activation (32). Interestingly, AHR in OX40$^{-/-}$ mice is markedly reduced (33). Thus, it is suggested that IL-1 functions in AHR through activating T_h2 cells.

IL-1 also potentiates T_h1 cell-mediated immune responses. APC-produced IL-1 induces CD40 ligand (L) (CD154) on CD4$^+$ T cells (26); cross-linking of CD40 on APC with CD40L leads to APC production of IL-12, IL-1α/β and TNF-α (34). These cytokines, including IL-1, all enhance the IL-12-dependent production of IFN-γ in BALB/c background mice (35). IL-4 production in IL-1RI$^{-/-}$ mice infected with *Leishmania major* increased from that seen in wild-type mice, suggesting IL-1 negatively regulates IL-4 expression (36). We found that the development of delayed-type hypersensitivity reaction,

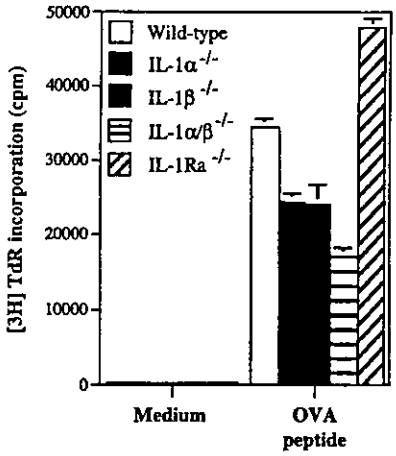

Fig. 6. OVA-specific T cell proliferative responses in IL-1α$^{-/-}$ and IL-1β$^{-/-}$ mice. The effects of IL-1 on T cell priming were evaluated using DO11.10 Tg T cells and splenic adherent cells from wild-type, IL-1α$^{-/-}$, IL-1β$^{-/-}$, IL-1α/β$^{-/-}$ and IL-1Ra$^{-/-}$ mice. The averages ± SD of triplicate experiments are shown. These results were reproduced in three independent experiments.

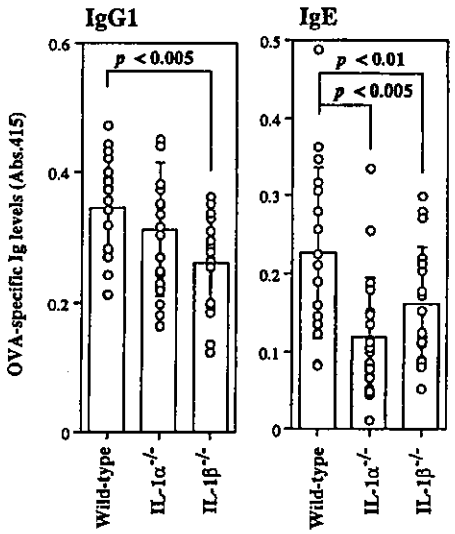

Fig. 7. OVA-specific IgG1 and IgE levels in sera from IL-1α$^{-/-}$ and IL-1β$^{-/-}$ mice during AHR. Sera were collected 24 h after the final inhalation. OVA-specific Ig levels were determined by ELISA. Both IgG1 and IgE levels specific to OVA in IL-1β$^{-/-}$ mice was low in comparison with the levels of wild-type mice, while IgE production in response to OVA was reduced only in IL-1α$^{-/-}$ mice. Each circle represents an individual mouse. An average and SD are shown. Wild-type (n = 17), IL-1α$^{-/-}$ (n = 17) and IL-1β$^{-/-}$ (n = 17) mice.

mediated by T_h1 cells, is significantly suppressed in IL-1α/β$^{-/-}$ mice on both the BALB/cA and C57BL/6J backgrounds, and that IL-1 is required for antigen-specific T_h1 cell activation (Nambu *et al.*, in preparation). Thus, IL-1 is likely involved in both T_h1 and T_h2 cell activation through the induction of the co-stimulatory molecules, CD40L and OX40, on CD4$^+$ T cells.

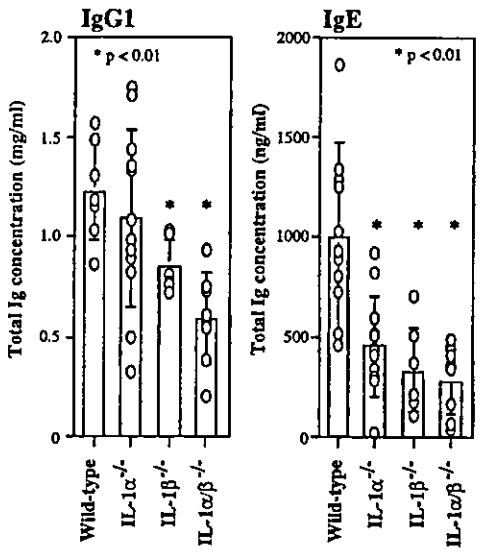

Fig. 8. Total IgG1 and IgE levels in sera from non-sensitized IL-1$^{-/-}$ mice. Sera were collected from non-sensitized mice. Total IgG1 and IgE levels were determined by ELISA. Total Ig levels from non-sensitized IL-1$^{-/-}$ mice showed a similar tendency to OVA-specific Ig levels in sensitized mice shown in Fig. 7. Each circle represents an individual mouse. Averages ± SD are shown. Wild-type (n = 11), IL-1α$^{-/-}$ (n = 12), IL-1β$^{-/-}$ (n = 6) and IL-1α/β$^{-/-}$ (n = 8) mice. *P < 0.01 versus wild-type mice.

We previously demonstrated that IL-1β rather than IL-1α is required for T cell-dependent IgG production (20). Consistent with this observation, IgG1 production against OVA during AHR was reduced in IL-1β$^{-/-}$, but not IL-1α$^{-/-}$, mice. The total and OVA-specific IgE levels in both IL-1α$^{-/-}$ and IL-1β$^{-/-}$ mice, however, were reduced from the levels seen in wild-type mice. Follicular dendritic cells (FDC), which are critical in B cell Ig class switching within germinal centers, express IL-1β, but not IL-1α (37). This evidence supports the idea that IgG1 and IgE production is reduced in IL-1β$^{-/-}$ mice, despite a molecular mechanism favoring the reduction of IgE levels in IL-1α$^{-/-}$ mice. Lymphotoxin (LT)α$^{-/-}$ mice exhibit a lack of LN and Peyer's patch development, abnormal architecture of the spleen, and germinal center formation failure resulting from defects in the FDC network (38). In these mutant mice, Ig class switching in response to particle antigens, including sheep red blood cells, does not occur (38). When treated with repeated immunization with soluble protein antigen with adjuvant, Ig class switching to these antigens occurred normally in LTα$^{-/-}$ mice despite the absence of germinal centers in the spleen (39). Thus, Ig class switching can occur independent of the FDC network and germinal center formation under specific conditions in which excess cytokines are produced. FDC produce IL-1β, but not IL-1α (37), while T_h2 cells express IL-1α (17). Although evidence may be lacking, we speculate that IL-1α, derived from T_h2 cells, may have a distinct role in the regulation of IgE production functioning independently from the IL-1β derived from germinal center FDC.

In summary, we demonstrated that both IL-1α and IL-1β have critical roles in the development of AHR through the activation of T_h2 cells during the sensitization phase. These findings may be useful to develop novel therapeutics to treat asthma.

Acknowledgements

We thank all the members of the laboratory for their excellent animal care. This study was supported by grants from the Ministry of Education, Science, Sport and Culture of Japan, and the Ministry of Health and Welfare of Japan.

Abbreviations

ACh	acetylcholine
APC	antigen-presenting cell
AHR	airway hypersensitivity response
CD40L	CD40 ligand
DTHR	delayed-type hypersensitivity response
FDC	follicular dendritic cell
LN	lymph node
LT	lymphotoxin
IL-1Ra	IL-1 receptor antagonist
IL-1RI and IL-1RII	IL-1 receptor type I and type II
OVA	ovalbumin
TNF	tumor necrosis factor
VCAM	vascular cell adhesion molecule

References

1 Wills-Karp, M. 1999. Immunologic basis of antigen-induced airway hyperresponsiveness. *Annu. Rev. Immunol.* 17:255.
2 Walker, C., Kaegi, M. K., Braun, P. and Blaser, K. 1991. Activated T cells and eosinophilia in bronchoalveolar lavages from subjects with asthma correlated with disease severity. *J. Allergy Clin. Immunol.* 88:935.
3 Lloyd, C. M., Gonzalo, J. A., Coyle, A. J. and Gutierrez-Ramos, J. C. 2001. Mouse models of allergic airway disease. *Adv. Immunol.* 77:263.
4 Walter, D. M., McIntire, J. J., Berry, G., McKenzie, A. N., Donaldson, D. D., DeKruyff, R. H. and Umetsu, D. T. 2001. Critical role for IL-13 in the development of allergen-induced airway hyperreactivity. *J. Immunol.* 167:4668.
5 Wedemeyer, J., Tsai, M. and Galli, S. J. 2000. Roles of mast cells and basophils in innate and acquired immunity. *Curr. Opin. Immunol.* 12:624.
6 Foster, P. S., Hogan, S. P., Ramsay, A. J., Matthael, K. I. and Young, I. G. 1996. Interleukin 5 deficiency abolishes eosinophilia, airways hyperreactivity, and lung damage in a mouse asthma model. *J. Exp. Med.* 183:195.
7 Schleimer, R. P., Sterbinsky, S. A., Kaiser, J., Bickel, C. A., Klunk, D. A., Tomioka, K., Newman, W., Luscinskas, F. W., Gimbrone, M. A., Jr, McIntyre, B. W., *et al.* 1992. IL-4 induces adherence of human eosinophils and basophils but not neutrophils to endothelium. Association with expression of VCAM-1. *J. Immunol.* 148:1086.
8 Panettieri, R. A., Jr, Lazaar, A. L., Pure, E. and Albelda, S. M. 1995. Activation of cAMP-dependent pathways in human airway smooth muscle cells inhibits TNF-α-induced ICAM-1 and VCAM-1 expression and T lymphocyte adhesion. *J. Immunol.* 154:2358.
9 Hultner, L., Kolsch, S., Stassen, M., Kaspers, U., Kremer, J. P., Mailhammer, R., Moeller, J., Broszeit, H. and Schmitt, E. 2000. In activated mast cells, IL-1 up-regulates the production of several T_h2-related cytokines including IL-9. *J. Immunol.* 164:5556.
10 Stassen, M., Arnold, M., Hultner, L., Muller, C., Neudorfl, C., Reineke, T. and Schmitt, E. 2000. Murine bone marrow-derived mast cells as potent producers of IL-9: costimulatory function of IL-10 and kit ligand in the presence of IL-1. *J. Immunol.* 164:5549.
11 Sironi, M., Sciacca, F. L., Matteucci, C., Conni, M., Vecchi, A., Bernasconi, S., Minty, A., Caput, D., Ferrara, P., Colotta, F., *et al.* 1994. Regulation of endothelial and mesothelial cell function by interleukin-13: selective induction of vascular cell adhesion molecule-1 and amplification of interleukin-6 production. *Blood* 84:1913.
12 Spoelstra, F. M., Postma, D. S., Hovenga, H., Noordhoek, J. A. and Kauffman, H. F. 1999. Interferon-γ and interleukin-4 differentially regulate ICAM-1 and VCAM-1 expression on human lung fibroblasts. *Eur. Respir. J.* 14:759.
13 Bjornsdottir, U. S. and Cypcar, D. M. 1999. Asthma: an inflammatory mediator soup. *Allergy* 54:55.
14 Broide, D. H., Campbell, K., Gifford, T. and Sriramarao, P. 2000. Inhibition of eosinophilic inflammation in allergen-challenged, IL-1 receptor type 1-deficient mice is associated with reduced eosinophil rolling and adhesion on vascular endothelium. *Blood* 95:263.
15 Kurt-Jones, E. A., Hamberg, S., Ohara, J., Paul, W. E. and Abbas, A. K. 1987. Heterogeneity of helper/inducer T lymphocytes. I. Lymphokine production and lymphokine responsiveness. *J. Exp. Med.* 166:1774.
16 Dinarello, C. A. 1991. Interleukin-1 and interleukin-1 antagonism. *Blood* 77:1627.
17 Hüber, M., Beuscher, H. U., Rohwer, P., Kurrle, R., Rollinghoff, M. and Lohoff, M. 1998. Costimulation via TCR and IL-1 receptor reveals a novel IL-1α-mediated autocrine pathway of T_h2 cell proliferation. *J. Immunol.* 160:4242.
18 al-Ramadi, B. K., Welte, T., Fernandez-Cabezudo, M. J., Galadari, S., Dittel, B., Fu, X. Y. and Bothwell, A. L. 2001. The Src-protein tyrosine kinase Lck is required for IL-1-mediated costimulatory signaling in T_h2 cells. *J. Immunol.* 167:6827.
19 Lin, K. W., Chen, S. C., Chang, F. H., Kung, J. T., Hsu, B. R. and Lin, R. H. 2002. The roles of interleukin-1 and interleukin-1 receptor antagonist in antigen-specific immune responses. *J. Biomed. Sci.* 9:26.
20 Nakae, S., Asano, M., Horai, R. and Iwakura, Y. 2001. Interleukin-1β, but not interleukin-1α, is required for T-cell-dependent antibody production. *Immunology* 104:402.
21 Horai, R., Asano, M., Sudo, K., Kanuka, H., Suzuki, M., Nishihara, M., Takahashi, M. and Iwakura, Y. 1998. Production of mice deficient in genes for interleukin (IL)-1α, IL-1β, IL-1α/β, and IL-1 receptor antagonist shows that IL-1β is crucial in turpentine-induced fever development and glucocorticoid secretion. *J. Exp. Med.* 187:1463.
22 Murphy, K. M., Heimberger, A. B. and Loh, D. Y. 1990. Induction by antigen of intrathymic apoptosis of $CD4^+CD8^+TCR^{lo}$ thymocytes *in vivo*. *Science* 250:1720.
23 de Bie, J. J., Henricks, P. A., Cruikshank, W. W., Hofman, G., Nijkamp, F. P. and van Oosterhout, A. J. 1999. Effect of interleukin-16-blocking peptide on parameters of allergic asthma in a murine model. *Eur. J. Pharmacol.* 383:189.
24 Williams, C. M. and Galli, S. J. 2000. Mast cells can amplify airway reactivity and features of chronic inflammation in an asthma model in mice. *J. Exp. Med.* 192:455.
25 Hamelmann, E., Schwarze, J., Takeda, K., Oshiba, A., Larsen, G. L., Irvin, C. G. and Gelfand, E. W. 1997. Noninvasive measurement of airway responsiveness in allergic mice using barometric plethysmography. *Am. J. Respir. Crit. Care. Med.* 156:766.
26 Nakae, S., Asano, M., Horai, R., Sakaguchi, N. and Iwakura, Y. 2001. IL-1 enhances T cell-dependent antibody production through induction of CD40 ligand and OX40 on T cells. *J. Immunol.* 167:90.
27 Brewer, J. M., Conacher, M., Hunter, C. A., Mohrs, M., Brombacher, F. and Alexander, J. 1999. Aluminium hydroxide adjuvant initiates strong antigen-specific T_h2 responses in the absence of IL-4- or IL-13-mediated signaling. *J. Immunol.* 163:6448.
28 Sulakvelidze, I., Inman, M. D., Rerecich, T. and O'Byrne, P. M. 1998. Increases in airway eosinophils and interleukin-5 with minimal bronchoconstriction during repeated low-dose allergen challenge in atopic asthmatics. *Eur. Respir. J.* 11:821.
29 Korsgren, M., Erjefalt, J. S., Korsgren, O., Sundler, F. and Persson, C. G. 1997. Allergic eosinophil-rich inflammation

develops in lungs and airways of B cell-deficient mice. *J. Exp. Med.* 185:885.
30 Takeda, K., Hamelmann, E., Joetham, A., Shultz, L. D., Larsen, G. L., Irvin, C. G. and Gelfand, E. W. 1997. Development of eosinophilic airway inflammation and airway hyperresponsiveness in mast cell-deficient mice. *J. Exp. Med.* 186:449.
31 Martin, T. R., Takeishi, T., Katz, H. R., Austen, K. F., Drazen, J. M. and Galli, S. J. 1993. Mast cell activation enhances airway responsiveness to methacholine in the mouse. *J. Clin. Invest.* 91:1176.
32 Lane, P. 2000. Role of OX40 signals in coordinating CD4 T cell selection, migration, and cytokine differentiation in T helper (T_h)1 and T_h2 cells. *J. Exp. Med.* 191:201.
33 Jember, A. G., Zuberi, R., Liu, F. T. and Croft, M. 2001. Development of allergic inflammation in a murine model of asthma is dependent on the costimulatory receptor OX40. *J. Exp. Med.* 193:387.
34 van Kooten, C. and Banchereau, J. 2000. CD40–CD40 ligand. *J. Leukoc. Biol.* 67:2.
35 Shibuya, K., Robinson, D., Zonin, F., Hartley, S. B., Macatonia, S. E., Somoza, C., Hunter, C. A., Murphy, K. M. and O'Garra, A. 1998. IL-1α and TNF-α are required for IL-12-induced development of T_h1 cells producing high levels of IFN-γ in BALB/c but not C57BL/6 mice. *J. Immunol.* 160:1708.
36 Satoskar, A. R., Okano, M., Connaughton, S., Raisanen-Sokolwski, A., David, J. R. and Labow, M. 1998. Enhanced T_h2-like responses in IL-1 type 1 receptor-deficient mice. *Eur. J. Immunol.* 28:2066.
37 Toellner, K. M., Scheel-Toellner, D., Sprenger, R., Duchrow, M., Trumper, L. H., Ernst, M., Flad, H. D. and Gerdes, J. 1995. The human germinal centre cells, follicular dendritic cells and germinal centre T cells produce B cell-stimulating cytokines. *Cytokine* 7:344.
38 Fu, Y. X., Molina, H., Matsumoto, M., Huang, G., Min, J. and Chaplin, D. D. 1997. Lymphotoxin-α (LTα) supports development of splenic follicular structure that is required for IgG responses. *J. Exp. Med.* 185:2111.
39 Matsumoto, M., Lo, S. F., Carruthers, C. J., Min, J., Mariathasan, S., Huang, G., Plas, D. R., Martin, S. M., Geha, R. S., Nahm, M. H. and Chaplin, D. D. 1996. Affinity maturation without germinal centres in lymphotoxin-α-deficient mice. *Nature* 382:462.

Impaired selectin-ligand biosynthesis and reduced inflammatory responses in β-1,4-galactosyltransferase-I–deficient mice

Masahide Asano, Susumu Nakae, Norihiro Kotani, Naoki Shirafuji, Aya Nambu, Noriyoshi Hashimoto, Hiroto Kawashima, Mayumi Hirose, Masayuki Miyasaka, Seiichi Takasaki, and Yoichiro Iwakura

Selectins recognize ligands containing carbohydrate chains such as sialyl Lewis x (sLe^x) that are mainly presented at the terminus of *N*-acetyl lactosamine repeats on core 2 *O*-glycans. Several glycosyltransferases act successively to extend the *N*-acetyl lactosamine repeats and to synthesize sLe^x, and β-1,4-galactosyltransferase (β4GalT) plays a key role in these processes. Recently isolated 6 *β4GalT* genes are candidates, but their individual roles, including those in selectin-ligand biosynthesis, remain to be elucidated. More than 80% of the core 2 *O*-glycans on the leukocyte membrane glycoproteins of β4GalT-I–deficient mice lacked galactose residues in β-1,4 linkage, and soluble P-selectin binding to neutrophils and monocytes of these mice was significantly reduced, indicating an impairment of selectin-ligand biosynthesis. β4GalT-I–deficient mice exhibited blood leukocytosis but normal lymphocyte homing to peripheral lymph nodes. Acute and chronic inflammatory responses, including the contact hypersensitivity (CHS) and delayed-type hypersensitivity (DTH) responses, were suppressed, and neutrophil infiltration into inflammatory sites was largely reduced in these mice. Our results demonstrate that β4GalT-I is a major galactosyltransferase responsible for selectin-ligand biosynthesis and that inflammatory responses of β4GalT-I–deficient mice are impaired because of the defect in selectin-ligand biosynthesis. (Blood. 2003;102: 1678-1685)

Introduction

The emigration of leukocytes to inflammatory sites during inflammation and infection, and the lymphocyte trafficking to lymph nodes (LNs) under normal circumstances progresses by means of sequentially acting cell adhesion molecules involved in leukocyte and endothelial cell interactions.[1] The initial event in this process is leukocyte rolling on the endothelial surface, which is mediated by selectins and their oligosaccharide ligands. Leukocyte emigration is known to be mediated by E- and P-selectin on endothelial cells and sialyl Lewis x (sLe^x) on leukocytes.[2,3] L-selectin on lymphocytes and sulfated sLe^x on the high endothelial venules (HEVs) of secondary lymphoid organs are involved in lymphocyte trafficking.[4,5] P-selectin recognizes both sLe^x and a core protein, P-selectin glycoprotein ligand-1 (PSGL-1),[6] whereas E- and L-selectin seem to bind oligosaccharide epitopes without a strict requirement for particular core proteins. However, the structure and biosynthesis of selectin oligosaccharide ligands remain to be elucidated.

Selectin ligands such as sLe^x and sulfated sLe^x are mainly expressed at the terminus of *N*-acetyl lactosamine repeats on serine/threonine (*O*)–Linked oligosaccharides (*O*-glycans).[7-9] In the biosynthesis of *O*-glycans, Galβ1→3GalNAcα1→Ser/Thr (core 1) is formed by the action of recently cloned core 1 β-1,3-galactosyltransferase[10] (core 1 β3GalT). Core 1 is then converted to GlcNAcβ1→6(Galβ1→3)GalNAcα1→Ser/Thr (core 2) by core 2 β-1,6-*N*-acetylglucosaminyltransferase (core 2 β6GnT) (Figure 1). Studies of core 2 β6GnT-deficient mice have revealed that core 2 *O*-glycans are essential for leukocyte emigration during inflammation but not for lymphocyte trafficking under normal circumstances.[11] These results suggest that most of the E- and P-selectin ligands are expressed on core 2 *O*-glycans. Recently, 6-sulfo sLe^x on extended core 1 *O*-glycans has been identified as one of the L-selectin ligands.[12] β-1,4-Galactosyltransferase (β4GalT) and β-1,3-*N*-acetylglucosaminyltransferase (β3GnT) act alternatively to extend *N*-acetyl lactosamine repeats on core 2 *O*-glycans, and β4GalT is also required to synthesize the sLe^x epitope in collaboration with α-2,3-sialyltransferase (ST) and α-1,3-fucosyltransferase (FucT) (Figure 1). Among these glycosyltransferases, Fuc-TVII has been shown to be mainly responsible for the fucosylation of sLe^x.[13,14] However, the contribution of the *β4GalT* genes in the biosynthesis of selectin ligands remains to be elucidated.

β4GalT is involved in the biosynthesis of biologically important galactose-containing oligosaccharides, such as stage-specific embryonic antigen-1 (SSEA-1 = Le^x), sLe^x, and 6-sulfo sLe^x. SSEA-1, which is expressed specifically on preimplantation embryos, has been suggested to play a role in morula compaction and blastocyst formation.[15] However, β4GalT-I–deficient embryos form normal compacted morulae and blastocysts. Polysialic acid (PSA) and human natural killer-1 (HNK-1) carbohydrate are expressed on the outer chains of the Galβ1→4GlcNAc-R backbone. These carbohydrates, which are expressed on neuronal cell adhesion

From the Department of Transgenic Animal Science, Graduate School of Medical Science, Kanazawa University; Center for Experimental Medicine, Department of Biochemistry, and Department of Advanced Medical Science, Institute of Medical Science, University of Tokyo; and Laboratory of Molecular and Cellular Recognition, Osaka University Graduate School of Medicine, Japan.

Submitted March 19, 2003; accepted April 19, 2003. Prepublished online as *Blood* First Edition Paper, April 24, 2003; DOI 10.1182/blood-2003-03-0836.

Supported in part by the Ministry of Education, Science, Sports and Culture of Japan (grants 10178104 and 13480280), the Inamori Foundation, and the Mochida Memorial Foundation for Medical and Pharmaceutical Research.

Reprints: Masahide Asano, Department of Transgenic Animal Science, Graduate School of Medical Science, Kanazawa University, 13-1 Takaramachi, Kanazawa 920-8640, Japan; e-mail: asano@kiea.m.kanazawa-u.ac.jp.

The publication costs of this article were defrayed in part by page charge payment. Therefore, and solely to indicate this fact, this article is hereby marked "advertisement" in accordance with 18 U.S.C. section 1734.

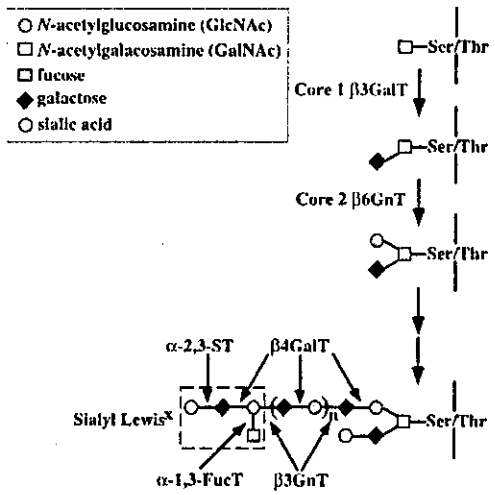

Figure 1. Biosynthesis of core 1 and core 2 *O*-glycans. Core 2 β6GnT generates a biantennary structure in *O*-glycans, and sLe^x is synthesized at the terminus of *N*-acetyl lactosamine disaccharide repeats on the core 2 branch. Core 1 β3GalT, core 1 β-1,3-galactosyltransferase; core 2 β6GnT, core 2 β-1,6-*N*-acetylglucosaminyltransferase; β4GalT, β-1,4-galactosyltransferase; α-1,3-FucT, α-1,3-fucosyltranferase; α-2,3-ST, α-2,3-sialyltransferase; β3GnT, β-1,3-*N*-acetylglucosaminyltransferase (I-extension enzyme).

proteins, are thought to be involved in neuronal cell recognition.[16,17] In support of this idea, we and another group showed that mice deficient in the biosynthesis of HNK-1 and PSA exhibit impaired synaptic plasticity, respectively.[18,19] To elucidate the biologic relevance of these galactose residues and their outer chains, we and another group previously generated β4GalT-I–deficient mice.[20,21] These mice exhibit growth retardation and semi-lethality before weaning because of the augmented proliferation and abnormal differentiation of small intestinal epithelial cells.[20] In contrast, PSA and HNK-1 are expressed normally, and no neuronal defects are detected in β4GalT-I–deficient mice,[22] suggesting that a *β4GalT* gene(s) other than *β4GalT-I* is responsible for the biosynthesis of PSA and HNK-1. Although approximately half the β4GalT-I–deficient mice die before the weaning period, the rest can be used for further study. In the present study, selectin-ligand biosynthesis and the effect of selectin-ligand deficiency were examined in β4GalT-I–deficient mice.

Seven *β4GalT* genes (*β4GalT-I* to *-VII*) have been isolated thus far,[23] and their individual roles, including those in selectin-ligand biosynthesis, remain to be elucidated. Because β4GalT-VII acts on xylose, β4GalT-I to –VI can catalyze the Galβ1→4GlcNAc linkage and thus are good candidates for the synthesis of selectin ligands such as sLe^x and 6-sulfo sLe^x.[23] Here, to evaluate the contribution of β4GalT-I in selectin-ligand biosynthesis, the carbohydrate structures of leukocytes from β4GalT-I–deficient mice and the inflammatory responses of these mice were examined. More than 80% of the core 2 *O*-glycans on the leukocyte membrane glycoproteins of β4GalT-I–deficient mice lacked galactose residues in β-1,4 linkage, and the binding of soluble P-selectin to the neutrophils and monocytes of β4GalT-I–deficient mice was reduced. These results indicate that selectin-ligand biosynthesis was severely impaired in β4GalT-I–deficient mice. Furthermore, β4GalT-I–deficient mice exhibited peripheral blood leukocytosis and reduced acute and chronic inflammatory responses, including contact hypersensitivity (CHS) and delayed-type hypersensitivity (DTH) responses, indicating a selectin-ligand deficiency. Our results clearly demonstrate that among the *β4GalT* gene family, β4GalT-I is a major galactosyltransferase responsible for selectin-ligand biosynthesis.

Materials and methods

β4GalT-I–deficient mice

The generation of β4GalT-I–deficient mice was described previously.[20] *β4GalT-I*$^{-/-}$ mice on a mixed background between 129/Sv and C57BL/6 were used for the experiments, with *β4GalT-I*$^{+/-}$ littermates as controls. Carbohydrate structures of the serum glycoproteins between *β4GalT-I*$^{+/+}$ and *β4GalT-I*$^{+/-}$ mice were indistinguishable,[24] and no overt phenotypes were observed in the *β4GalT-I*$^{+/-}$ mice. The mice were kept under specific pathogen-free conditions in an environmentally controlled clean room at the Laboratory Animal Research Center, Institute of Medical Science, University of Tokyo and at the Institute for Experimental Animals, Kanazawa University. Experiments were conducted according to institutional ethical guidelines for animal experiments and safety guidelines for gene manipulation experiments.

Preparation of *O*-glycans from splenocytes

Splenocytes were prepared by grinding the spleen with the plunger of a disposable syringe, passing the ground spleen through nylon mesh, and suspending the cells in minimum essential medium (MEM). They were then treated twice with hemolysis buffer (17 mM Tris-HCl containing 140 mM NH_4Cl, pH 7.2) to remove red blood cells and were passed through nylon mesh to remove debris. The cells were washed twice with phosphate-buffered saline (PBS), homogenized in 10 mM Tris-HCl containing 1 mM EDTA (ethylenediaminetetraacetic acid), pH 7.4 (TE buffer), and spun at 150*g* for 5 minutes. The supernatant was spun at 25 000*g* for 30 minutes, and the precipitate was washed twice with TE buffer and once with 10 mM ammonium acetate. The precipitated membrane fraction was lyophilized and delipidated as previously described.[25] Delipidated ghosts were suspended in 1 mL 0.05 M NaOH containing 1 M sodium borohydride and were incubated at 45°C for 16 hours. Released glycans were purified according to the method described previously.[26]

Analysis of *O*-glycans by HPAEC-PAD

High-pH anion-exchange chromatography with pulsed amperometric detection (HPAEC-PAD) was performed using a Bio-LC system (Dinex, Sunnyvale, CA) equipped with a CarboPac PA-1 column (4 × 250 mm) and a pulsed amperometric detector. *O*-glycans were eluted with a linearly increasing concentration of 0 to 400 mM sodium acetate in 100 mM NaOH from 0 to 30 minutes. *O*-glycans were also desialylated by mild acid hydrolysis with 0.01 M HCl at 100°C for 20 minutes and analyzed by HPAEC-PAD using an isocratic elution with 22 mM NaOH.

Flow cytometric analysis

Splenocytes were prepared as described above except that they were treated with the hemolysis buffer only once. Splenocytes (2×10^6 cells) were blocked with antimouse CD16/CD32 for 15 minutes and were incubated with the first antibody or human–P-selectin immunoglobulin M (IgM) for 45 minutes. When antirat IgG2b was used as the second antibody, mouse serum was used for blocking instead of antimouse CD16/CD32. The splenocytes were washed, incubated with R-phycoerythrin (PE)– or fluorescein isothiocyanate (FITC)–conjugated second antibodies for 45 minutes, washed again, and incubated with 7-amino actinomycin D (Sigma, St Louis, MO). Incubations with antibodies were carried out on ice. Data were analyzed on a FACScan flow cytometer using Lysis II software (Becton Dickinson, Mountain View, CA).

A human P-selectin–IgM expression plasmid, human P-selectin–IgM/pcDNA1.1, which bears part of the human P-selectin cDNA containing the NH_2-terminal lectin domain, the epidermal growth factor (EGF)–like domain, and the first 2 complement-binding protein-like domains (provided by Ono Pharmaceutical, Osaka, Japan), and the μ heavy chain of human

IgM (provided by Dr A. Traunecker, Basel Institute for Immunology, Switzerland) was transfected into human embryonic kidney-derived 293T cells (provided by Dr Y. Kanakura, Osaka University Graduate School of Medicine, Japan). The pAdVAntage vector (Promega, Madison, WI) was cotransfected with human P-selectin–IgM/pcDNA1.1 to enhance protein expression levels. Four days after transfection, the culture medium containing the P-selectin–IgM was collected and stored at −80°C until use.

Antimouse CD16/CD32 (2.4G2), antimouse Gr-1 (RB6-8C5), and antimouse PSGL-1 (2PH1), were purchased from PharMingen (San Diego, CA). PE-antimouse F4/80 and FITC-antirat IgG were purchased from Caltag (Burlingame, CA), and FITC-antihuman IgM was purchased from American Qualex (San Clemente, CA). PE-antirat IgG was kindly provided by Dr T. Yoshimoto (Institute for Medical Sciences, University of Tokyo, Japan).

Colony-forming activity of bone marrow cells

Nonadherent mononuclear cells (1×10^4) were prepared from the bone marrow of *β4GalT-I*$^{-/-}$ (n = 5) and *β4GalT-I*$^{+/-}$ (n = 5) mice (2-3 months old) and plated into 0.45% methylcellulose in the presence of 50 ng/mL granulocyte–colony-stimulating factor (G-CSF) (provided by Chugai Pharmaceutical, Tokyo, Japan), 2 U/mL EPO (provided by Kirin Brewery, Tokyo, Japan), or 20 ng/mL interleukin-3 (IL-3; Amgen, Thousand Oaks, CA). Colonies were counted after 2 weeks.

Acute inflammation

Zymosan-induced inflammation was carried out as described previously.[27] *β4GalT-I*$^{-/-}$ (n = 10) and *β4GalT-I*$^{+/-}$ (n = 8) mice were anesthetized with ketamine and xylazine, and 20 μL 2% zymosan A (Sigma) and saline were injected subcutaneously into the right and left earlobes, respectively, using a microsyringe (Hamilton, Reno, NV) with a 30-gauge needle. At 8 hours after the injection, when the swelling reached peak levels, the mice were killed, and a disk of each earlobe was removed using a 6-mm biopsy punch and weighed. Ear swelling was calculated as follows: [Increase of ear swelling (%)] = ([weight of challenged earlobe] − [weight of vehicle-treated earlobe]) × 100/[weight of vehicle-treated earlobe].

CHS response

β4GalT-I$^{-/-}$ (n = 11) and *β4GalT-I*$^{+/-}$ (n = 11) mice were sensitized by the epicutaneous application of 100 μL 7% 2,4,6-trinitrochlorobenzene (TNCB) (Tokyo Chemical, Tokyo, Japan) in acetone/olive oil (3:1, vol/vol) onto shaved abdomens. On day 5 after sensitization, 20 μL 1% TNCB solution and the solvent alone were applied epidermally onto the right and left earlobe, respectively. Mice were killed, and earlobe biopsies were taken as described above 24 hours after the second challenge, when the swelling reached peak levels. Each ear disk was weighed, and the ear swelling was calculated as described above.

DTH response

β4GalT-I$^{-/-}$ (n = 8) and *β4GalT-I*$^{+/-}$ (n = 8) mice were sensitized by the subcutaneous injection of 200 μL 1.25 mg/mL methylated bovine serum albumin (mBSA) (Sigma) in PBS/complete Freund adjuvant (1:1, vol/vol) into the tail roots. On day 7 after the sensitization, 20 μL 10 mg/mL mBSA in PBS and PBS alone were applied epidermally onto the right and left footpad, respectively. Mice were killed, and footpad thickness was measured 24 hours after the second challenge, when the swelling reached peak levels. Footpad thickness was calculated as follows: [Increase of footpad thickness (%)] = ([thickness of challenged footpad] − [thickness of vehicle-treated footpad]) × 100/[thickness of vehicle-treated footpad].

Histology

Tissues were fixed in 10% neutral formalin, dehydrated, and embedded in paraffin wax according to standard procedures. Footpads were defatted with methanol and chloroform (1:1) and were decalcified with 5% formic acid before they were embedded in paraffin wax. Sections of 6 μm were made and stained with Weigert hematoxylin-eosin.

Myeloperoxidase assay

Ear disks (obtained with a 6-mm punch) were homogenized in 400 μL PBS and sonicated for 30 seconds. The homogenates were frozen and thawed 3 times and again were sonicated for 30 seconds. After the debris was removed by centrifugation, myeloperoxidase (MPO) activity in the supernatants was measured as described.[28] The MPO assay was carried out in 400 μL 50 mM potassium-phosphate buffer (pH 6.0) containing 0.4 mg/mL *O*-phenylenediamine (Sigma) and 0.05% H_2O_2 for 20 minutes. The reaction was stopped by the addition of 100 μL 0.4 M H_2SO_4, and OD 490 nm was measured. MPO activity was calculated using commercial peroxidase (Sigma) as a standard.

Statistical analysis

Statistical evaluation was carried out by means of the Student *t* test or the Welch *t* test according to the Levene test for equality of variance between β4GalT-I–deficient and control mice. A 2-sided level of $P < .05$ was accepted as statistically significant. Data are presented as mean ± SEM.

Results

Biosynthesis of *O*-glycans on β4GalT-I–deficient leukocytes

Sialyl Le^x is most abundantly expressed at the terminus of *N*-acetyl lactosamine disaccharide repeats on core 2 *O*-glycans.[3] As shown in Figure 1, a *β4GalT* gene must be involved in the biosynthesis of the *N*-acetyl lactosamine disaccharide repeats and terminal sLe^x epitope on the core 2 branch. To clarify the contribution of the *β4GalT-I* gene in the core 2 *O*-glycan biosynthesis on leukocytes, the *O*-glycan structures of splenocyte membrane glycoproteins prepared from *β4GalT-I*$^{+/-}$ and *β4GalT-I*$^{-/-}$ mice were analyzed by HPAEC-PAD.

Eight major glycan peaks were detected in samples from the *β4GalT-I*$^{+/-}$ mice, and 6 major peaks were seen in samples from the *β4GalT-I*$^{-/-}$ mice (Figure 2A-B). Considering their elution positions compared with those of authentic *O*-glycan standards from fetuin, sheep erythrocytes, erythrocytes from *β4GalT-I*$^{-/-}$ mice,[25,26] and their previous structural analysis,[26] we deduced the structures giving rise to each peak to be those shown in Figure 2C. Thus, the glycans with β1,4-galactosylated core 2 branch structures corresponding to peaks 4, 6, and 8 in the *β4GalT-I*$^{+/-}$ sample were only faintly detected or not detected in the *β4GalT-I*$^{-/-}$ sample, and a glycan with an abnormal core 2 branch that lacked galactose residues in β-1,4 linkage (peak 2) was abundantly detected in the *β4GalT-I*$^{-/-}$ sample. In contrast, core 1 *O*-glycans were equally synthesized in both mice.

To further confirm the impaired β1,4-galactosylation of core 2 branches in the *β4GalT-I*$^{-/-}$ sample, the *O*-glycans of splenocyte membrane glycoproteins were mildly hydrolyzed to remove sialic acids and were analyzed by HPAEC-PAD. The resultant asialo *O*-glycans from the *β4GalT-I*$^{+/-}$ sample gave 2 peaks corresponding to a core 1 disaccharide, Galβ1→3GalNAc-ol (70%), and a core 2 tetrasaccharide, Galβ1→3(Galβ1→4GlcNAcβ1→6)GalNAc-ol (30%) (Figure 3A). In contrast, the similarly treated sample from *β4GalT-I*$^{-/-}$ mice was composed of the core 1 disaccharide (72%), a core 2 trisaccharide, Galβ1→3(GlcNAcβ1→6)GalNAc-ol (24%), and the core 2 tetrasaccharide (4.0%) (Figure 3B). The peak area ratio of the core 1 disaccharide was nearly the same for both mice. However, the core 2 tetrasaccharide was dramatically reduced for the *β4GalT-I*$^{-/-}$ mice. The ratio of core 2 trisaccharide (β1,4-ungalactosylated) to the tetrasaccharide (β1,4-galactosylated) revealed that most (86%) core 2 branch lacked galactose residues in β-1,4 linkage in the leukocytes of *β4GalT-I*$^{-/-}$ mice, as

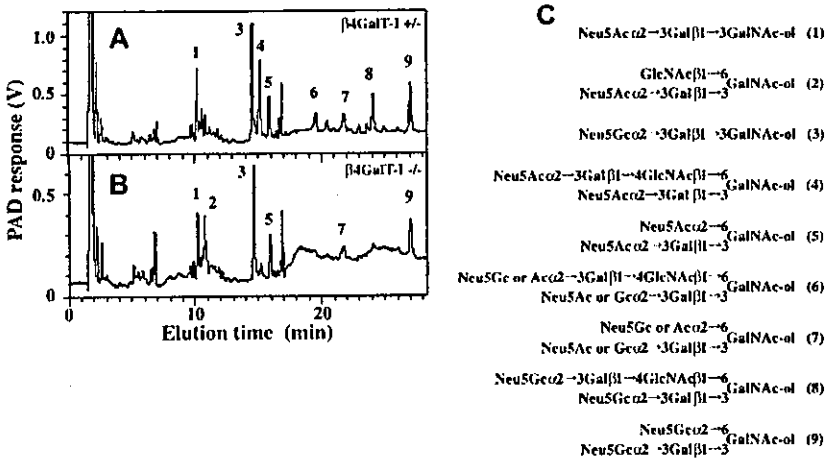

Figure 2. Analysis of *O*-glycans by HPAEC-PAD. Glycans released by alkaline-borohydride treatment from delipidated splenocyte membrane glycoproteins were analyzed by HPAEC-PAD. (A) *β4GalT-I*$^{+/-}$ splenocytes. (B) *β4GalT-I*$^{-/-}$ splenocytes. (C) Proposed structures of the *O*-glycans (A-B). The major glycan peaks are numbered in panels A and B, and the numbers in parentheses in panel C represent the peak numbers in panels A and B.

had also been observed in their erythrocytes.[25] These results clearly indicate that β4GalT-I plays a central role in the formation of the galactosylated core 2 branch, which is a prerequisite for further elongation of the polylactosamine chains.

Selectin-ligand formation on β4GalT-I–deficient neutrophils and monocytes

Selectin-ligand formation on the surface of neutrophils and monocytes from *β4GalT-I*$^{-/-}$ mice was analyzed by flow cytometry using a chimeric human P-selectin IgM molecule. The binding of P-selectin to splenic neutrophils (Gr-1–positive) and splenic monocytes (F4/80-positive) was markedly reduced in *β4GalT-I*$^{-/-}$ mice compared with *β4GalT-I*$^{+/-}$ mice (Figure 4). Because PSGL-1 is the predominant ligand for P-selectin on neutrophils,[29] the expression of PSGL-1 on neutrophils and monocytes was compared between *β4GalT-I*$^{-/-}$ and *β4GalT-I*$^{+/-}$ mice and was found to be the same (Figure 4C). These data, together with the impaired core 2 *O*-glycan biosynthesis, indicate that the biosynthesis of the selectin-ligand oligosaccharide is severely reduced, though not completely abrogated, in β4GalT-I–deficient neutrophils and monocytes.

Leukocytosis and neutrophilia of β4GalT-I–deficient mice

Leukocytosis and neutrophilia are commonly observed in selectin-deficient mice and selectin ligand-deficient mice.[11,13,14,30] Here, the total white blood cell count in the peripheral blood was elevated 2.2-fold in the *β4GalT-I*$^{-/-}$ mice compared with the *β4GalT-I*$^{+/-}$ mice (Figure 5A, Table 1). Neutrophil and lymphocyte counts were also increased 2.3-and 2.5-fold, respectively (Figure 5B, Table 1). Therefore, β4GalT-I–deficient mice also showed leukocytosis and neutrophilia.

To clarify whether leukocytosis was caused by abnormal hematopoiesis in the bone marrow, the colony-forming activity of bone marrow cells was measured. Colony-forming units (CFUs) in the presence of G-CSF or IL-3 were comparable between *β4GalT-I*$^{-/-}$ and *β4GalT-I*$^{+/-}$ mice, suggesting that the hematopoietic differentiation of β4GalT-I–deficient bone marrow cells into the leukocyte lineage was normal (Figure 5C). In contrast, CFUs in the presence of EPO were significantly increased in the *β4GalT-I*$^{-/-}$ mice (Figure 5C). Red blood cell counts, hematocrit values, and hemoglobin concentrations in the peripheral blood were slightly but significantly reduced in the *β4GalT-I*$^{-/-}$ mice (Figure 5A). The high response to EPO might have been attributed to the mild anemia observed in the *β4GalT-I*$^{-/-}$ mice.

In addition to peripheral blood leukocytosis, splenomegaly and extramedullary hematopoiesis in the spleen and liver were often

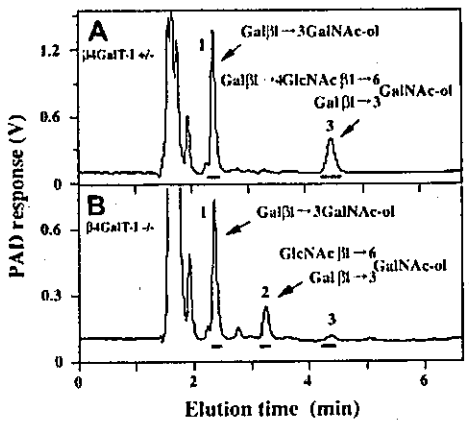

Figure 3. Analysis of desialylated *O*-glycans by HPAEC-PAD. Desialylated *O*-glycans from splenocyte membrane glycoproteins were analyzed by HPAEC-PAD. (A) *β4GalT-I*$^{+/-}$ splenocytes. (B) *β4GalT-I*$^{-/-}$ splenocytes. The major glycan peaks are numbered (A-B), and their proposed structures are given in the figure.

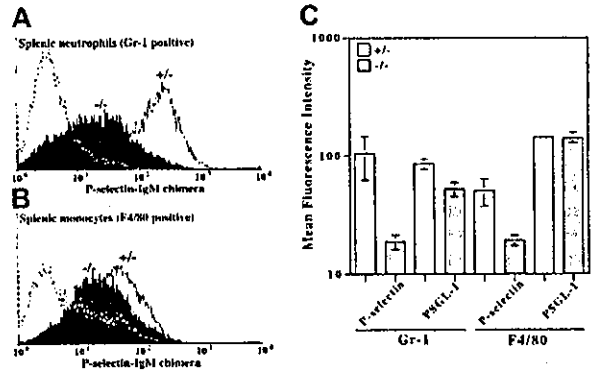

Figure 4. Binding of P-selectin and PSGL-1 to neutrophils and monocytes. Binding of the human–P-selectin IgM chimeric molecule and PSGL-1 to splenic neutrophils (Gr-1 gated) and splenic monocytes (F4/80 gated) was analyzed by flow cytometry. (A) Neutrophils from the spleens of *β4GalT-I*$^{+/-}$ (open histogram) and *β4GalT-I*$^{-/-}$ (filled histogram) mice. The dotted line shows negative control without the P-selectin–human IgM chimeric molecule. Results from 1 of 3 representative experiments are shown. (B) Monocytes from the spleens of *β4GalT-I*$^{+/-}$ and *β4GalT-I*$^{-/-}$ mice as in panel A. Results from 1 of 2 representative experiments are shown. (C) Mean fluorescence intensities of P-selectin binding and PSGL-1 expression in splenic neutrophils (Gr-1 gated; n = 3) and splenic monocytes (F4/80 gated; n = 2). Data are presented as means ± SEM.

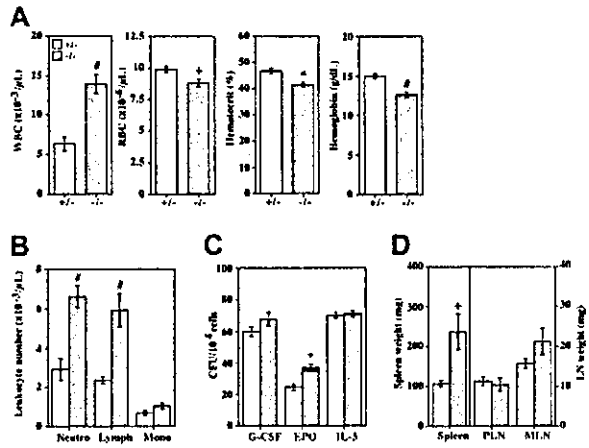

Figure 5. Peripheral blood hematology and the colony-forming activity of bone marrow cells. (A) Total white blood cell counts, red blood cell counts, hematocrit values, and hemoglobin concentrations of the peripheral blood from *β4GalT-I*$^{+/-}$ (□; n = 6) and *β4GalT-I*$^{-/-}$ mice (□; n = 6) at 2 to 3 months of age were measured by an automatic cell counter. (B) Numbers of neutrophils, lymphocytes, and monocytes from *β4GalT-I*$^{+/-}$ (□; n = 6) and *β4GalT-I*$^{-/-}$ (□; n = 6) mice were measured manually. (C) CFUs of nonadherent mononuclear cells (1 × 10^4) prepared from the bone marrow of *β4GalT-I*$^{+/-}$ (□, n = 5) and *β4GalT-I*$^{-/-}$ (□; n = 5) mice were measured in the presence of 50 ng/mL G-CSF, 2 U/mL EPO, or 20 ng/mL IL-3. (D) Weights of spleens, PLNs (cervical LN + axillary LN), and mesenteric (M) LNs were compared between *β4GalT-I*$^{+/-}$ (□; n = 9) and *β4GalT-I*$^{-/-}$ (□; n = 8) mice at 2 to 4.5 months of age. #$P < .005$; *$P < .01$; +$P < .05$. Data are presented as means ± SEM.

observed in the β4GalT-I–deficient mice (Figure 5D and data not shown). Microscopic observation of spleen and liver sections showed extramedullary hematopoiesis, including the presence of erythroid precursors, granulocytes, and megakaryocytes, in the *β4GalT-I*$^{-/-}$ mice (data not shown).

Normal lymphocyte homing to peripheral lymph nodes

Lymphocyte homing to peripheral lymph nodes (PLNs) is mediated by L-selectin on lymphocytes and L-selectin ligands, such as 6-sulfo sLe^x on the HEVs of PLNs. *β4GalT-I*$^{-/-}$ mice had cervical, axillary, and mesenteric LNs that were comparable in weight to those of *β4GalT-I*$^{+/-}$ mice (Figure 5D). In addition, an in vivo lymphocyte homing assay using 5-chloromethylfluorescein diacetate (CMFDA)–labeled wild-type lymphocytes[13] demonstrated that lymphocyte trafficking to PLNs was normal in *β4GalT-I*$^{-/-}$ mice (data not shown). These results suggest that lymphocyte homing to PLNs was not affected in the β4GalT-I–deficient mice.

Acute inflammation of β4GalT-I–deficient mice

Cell adhesion through selectins and their ligands plays an important role in acute and chronic inflammation. Zymosan-induced

Table 1. Comparison of leukocytosis and neutrophilia between selectin-perturbed KO mice

Blood cell types	Fold increase in cell numbers compared with control mice				
	β4GalT-1 KO	Core 2 β6GnT KO	E/P-selectin KO	Fuc-TVII KO	Fuc-TIV/VII KO
Leukocytes	2.2	2.4	3.9	3.2	2.9
Neutrophils	2.3	4.3	16.6	7.4	16.4
Lymphocytes	2.5	1.6	1.5	2.0	1.2
Monocytes	1.6	1.4	9.8	2.9	4.2

Data are from core 2 β6GnT-deficient mice,[11] E- and P-selectin double-deficient mice,[30] Fuc-TVII-deficient mice,[13] and Fuc-TIV/VII double-deficient mice.[14]
KO indicates knockout.

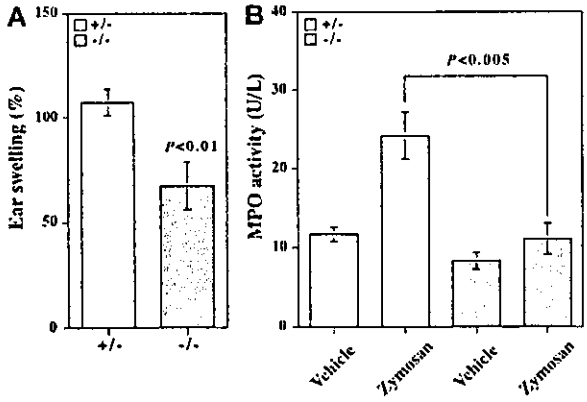

Figure 6. Neutrophil trafficking during acute inflammation. (A) Zymosan-induced dermatitis. Earlobes of *β4GalT-I*$^{+/-}$ (□; n = 8) and *β4GalT-I*$^{-/-}$ (□; n = 10) mice were injected subcutaneously with zymosan (right ear) or saline (left ear), and the weight of each earlobe disk was measured after 6 hours. Ear swelling was calculated as described in "Materials and methods." (B) MPO activity in the earlobe homogenates was measured. Data are presented as means ± SEM.

dermatitis is a model in which acute inflammation is mediated by E- and P-selectins.[27] Zymosan-induced ear swelling was significantly, but not completely, suppressed in *β4GalT-I*$^{-/-}$ mice compared with *β4GalT-I*$^{+/-}$ mice (Figure 6A). Neutrophil trafficking into the inflamed earlobe as measured by MPO activity was not induced by the zymosan treatment in *β4GalT-I*$^{-/-}$ mice, whereas in *β4GalT-I*$^{+/-}$ mice it was induced 2-fold (Figure 6B). Therefore, acute inflammation induced by zymosan was significantly suppressed in the β4GalT-I–deficient mice, probably because of a defect in neutrophil trafficking.

CHS and DTH responses of β4GalT-I–deficient mice

CHS is a typical chronic cutaneous inflammation in which selectins are known to be involved.[31] TNCB was applied epidermally onto the earlobe 5 days after sensitization by the epicutaneous application of TNCB onto the abdomen. The increase in ear swelling 24 hours after the second challenge was significantly, but not completely, suppressed in *β4GalT-I*$^{-/-}$ mice compared with *β4GalT-I*$^{+/-}$ mice (Figure 7A). In addition, neutrophil trafficking as measured by MPO activity after the sensitization was also reduced in the *β4GalT-I*$^{-/-}$ mice (Figure 7B).

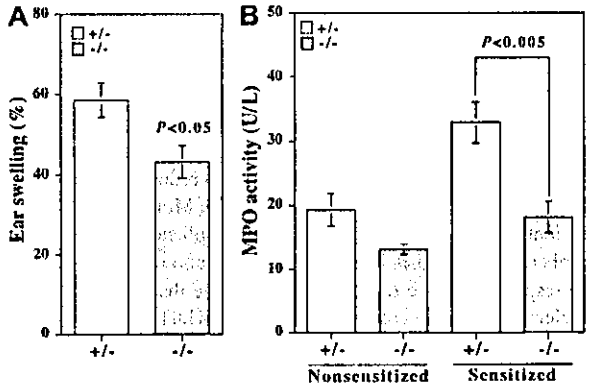

Figure 7. CHS response induced by TNCB. (A) CHS response was induced by TNCB in TNCB-sensitized *β4GalT-I*$^{+/-}$ (□; n = 11) and *β4GalT-I*$^{-/-}$ (□; n = 11) mice. Ear swelling was calculated as described in "Materials and methods." (B) MPO activity in the CHS-induced earlobe. TNCB-sensitized or nonsensitized *β4GalT-I*$^{+/-}$ (□) and *β4GalT-I*$^{-/-}$ (□) mice were treated with TNCB, and the MPO activity in the earlobe homogenates was measured. Data are presented as means ± SEM.

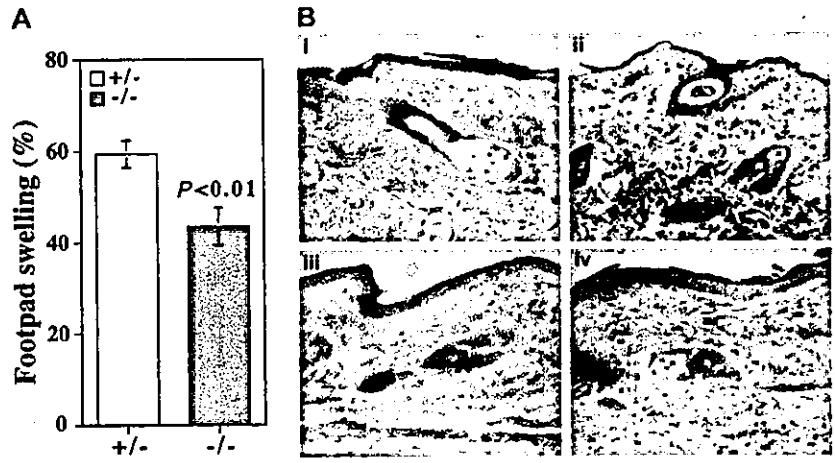

Figure 8. DTH response induced by mBSA. (A) DTH response was induced by mBSA in mBSA-sensitized *β4GalT-I*$^{+/-}$ (□; n = 8) and *β4GalT-I*$^{-/-}$ (■; n = 8) mice. The increase in footpad thickness was calculated as described in "Materials and methods." (B) Weigert hematoxylin and eosin staining of footpad sections. (i) PBS-injected *β4GalT-I*$^{+/-}$ mice. (ii) mBSA-injected *β4GalT-I*$^{+/-}$ mice. (iii) PBS-injected *β4GalT-I*$^{-/-}$ mice. (iv) mBSA-injected *β4GalT-I*$^{-/-}$ mice. Original magnification, × 100.

Although CHS was once thought to be a prototypic DTH response, recent reports indicate that CHS and DTH are mediated by major histocompatibility complex (MHC) class 1-restricted CD8$^+$ T cells and MHC class 2-restricted CD4$^+$ T cells, respectively.[32] The mBSA-induced DTH responses were compared between the β4GalT-I–deficient and control mice. An increase in footpad thickness induced by the epicutaneous application of mBSA after sensitization was significantly, but not completely, suppressed in *β4GalT-I*$^{-/-}$ mice compared with *β4GalT-I*$^{+/-}$ mice (Figure 8A). Leukocyte infiltration into the dermis of the footpad was induced by the mBSA treatment in *β4GalT-I*$^{+/-}$ mice, but it was suppressed in *β4GalT-I*$^{-/-}$ mice (Figure 8B). Therefore, chronic inflammation such as CHS and DTH was also suppressed in the β4GalT-I–deficient mice.

Discussion

Biosynthesis of *O*-glycans and selectin ligands in β4GalT-I–deficient mice

β4GalT-I was thought to be mainly involved in the biosynthesis of Galβ1→4GlcNAc units in *N*-glycans and in lactose synthesis through binding with α-lactalbumin in the mammary gland.[33] Our previous and present studies demonstrated that β4GalT-I is also responsible for the biosynthesis of core 2 *O*-glycans, given that core 2 *O*-glycan biosynthesis was reduced by more than 80% in the erythrocytes[25] and leukocytes of β4GalT-I–deficient mice. Given that selectin ligands such as sLe^x and 6-sulfo sLe^x are mainly expressed on the core 2 branch of *O*-glycans,[3] selectin ligand expression would be expected to be reduced in β4GalT-I–deficient mice. As shown in Figure 4, the binding of β4GalT-I–deficient neutrophils and monocytes to P-selectin was reduced in these mice, though PSGL-1 expression was not affected. Moreover, β4GalT-I–deficient mice showed selectin-deficient phenotypes, including peripheral leukocytosis and impaired acute and chronic inflammatory responses. These results clearly indicate that the biosynthesis of selectin ligands is greatly impaired in β4GalT-I–deficient mice.

Seven *β4GalT* genes have been isolated, and 6 of them are candidates for the biosynthesis of *O*-glycans and selectin ligands.[23] Using purified β4GalT enzymes and synthetic oligosaccharide acceptors, Ujita et al demonstrated that β4GalT-IV synthesized the core 2 branch most efficiently, whereas β4GalT-I was involved in the biosynthesis of the core 4 branch in *O*-glycans biosynthesis.[34,35] These findings are not consistent with our results. The *N*-acetyl lactosamine extension activity in core 2 and core 4 *O*-glycans was compared among the β4GalTs using various synthetic acceptors in their in vitro experiments. However, the in vivo situation could be different from that of the in vitro study, which used large amounts of purified β4GalTs and synthetic oligosaccharide acceptors instead of glycoproteins. Because the expression level of each *β4GalT* gene differs according to cell type, the biosynthesis of the core 2 branch of *O*-glycans could be carried out by different *β4GalT* genes in different cell types. We examined the biosynthesis of core 2 *O*-glycans in leukocytes, where selectin ligands are synthesized. Therefore, β4GalT-I definitely contributes to and plays a major role in the biosynthesis of the core 2 branch of *O*-glycans and selectin ligands in living leukocytes.

Given that approximately 20% of the core 2 branches were galactosylated by a β-1,4 linkage and that P-selectin bound weakly to neutrophils and monocytes in β4GalT-I–deficient mice, other *β4GalT* gene(s), such as *β4GalT-IV*, must be involved in the biosynthesis of the core 2 branch of *O*-glycans and selectin ligands. Recently, it has been reported that β4GalT-IV is involved in the biosynthesis of 6-sulfo sLe^x, an L-selectin ligand.[36] To identify the other *β4GalT* gene or genes responsible for selectin-ligand biosynthesis, mice deficient in those genes will have to be analyzed.

Peripheral leukocytosis and normal lymphocyte homing to PLNs in β4GalT-I–deficient mice

β4GalT-I–deficient mice exhibited peripheral leukocytosis and neutrophilia similar to those seen in selectin- and selectin-ligand–deficient mice, strongly suggesting that β4GalT-I–deficient mice are impaired in selectin-dependent endothelial cell adhesion. A comparison of the β4GalT-I–deficient mice with selectin-deficient mice and other glycosyltransferase-deficient mice is shown in Table 1. E- and P-selectin double-deficient mice exhibit severe leukocytosis and neutrophilia,[30] whereas P-selectin single-deficient mice show mild neutrophilia without leukocytosis[37] and L-selectin and E-selectin single-deficient mice show normal hematology.[38,39] Fuc-TIV/VII double-deficient mice also show severe leukocytosis and neutrophilia,[14] but those in core 2 β6GnT-deficient mice are milder.[11] The leukocytosis and neutrophilia of β4GalT-I–deficient mice were intermediate, comparable to those of core 2 β6GnT-deficient mice, which show a complete deficiency of core 2 *O*-glycans and a partial deficiency of selectin ligands.[11] β4GalT-I–deficient mice also showed considerable deficiency in core 2 *O*-glycans biosynthesis and a partial deficiency of selectin ligands.

Therefore, deficiency in the biosynthesis of core 2 *O*-glycans causes moderate leukocytosis and neutrophilia.

Normal hematopoietic activity of the bone marrow cells (Figure 5C) and extramedullary hematopoiesis in the spleen and liver (data not shown) suggest that leukocyte production was increased in the periphery in β4GalT-I–deficient mice, though increased hematopoiesis in the bone marrow cannot be ruled out completely. Subclinical infection will induce cytokine production and cause extramedullary hematopoiesis, similar to those observed in E- and P-selectin double-deficient mice.[30,40] Our β4GalT-I–deficient mice, however, were kept under specific pathogen-free (SPF) conditions, and no pathologic features, including the ulcerative cutaneous infection seen in the E- and P-selectin double-deficient mice, were observed. Therefore, the basal expression of E- and P-selectins and their oligosaccharide ligands is indispensable for the regulated production of leukocytes in the periphery, independent of infection. Altered leukocyte homeostasis might be caused by several mechanisms, as discussed previously.[30] One possibility is that tissue leukocytes are reduced because of a defect in selectin-dependent endothelial cell adhesion, causing an elevation of leukocytes in the blood. Another possibility is that neutrophilia may be caused by an increase in neutrophil half-life in the circulation, as reported in P-selectin–deficient mice.[41] Homeister et al[14] reported that extreme leukocytosis in Fuc-TIV/VII double-deficient mice is caused by decreased neutrophil turnover and increased neutrophil production in the periphery. Because epithelial cell proliferation is enhanced in β4GalT-I–deficient mice,[20] leukocyte proliferation might be augmented.

Lymphocyte homing to PLNs is mediated by L-selectin on lymphocytes and L-selectin ligands on the HEVs of PLNs. Indeed, lymphocyte homing is impaired in L-selectin–deficient mice[39] and in Fuc-TVII–deficient mice.[13] However, the weight of the PLNs and the in vivo lymphocyte homing activity were comparable between β4GalT-I–deficient and control mice (Figure 5D and data not shown). These results suggest that lymphocyte homing to PLNs was not affected in β4GalT-I–deficient mice, as is also observed in core 2 β6GnT-deficient mice.[11] Taken together, these observations indicate that core 2 *O*-glycans are dispensable for the biosynthesis of L-selectin ligands.

Reduced acute and chronic inflammatory responses in β4GalT-I–deficient mice

Cell adhesion through selectins and their oligosaccharide ligands is a prerequisite for leukocyte accumulation at inflammatory sites. Zymosan-induced inflammation is a model in which acute inflammation is mainly mediated by neutrophils. Zymosan-induced neutrophil recruitment is reduced in E- and P-selectin double-deficient mice[27] and fully compromised in Fuc-TIV/VII double-deficient mice.[14] These results indicate that E- and P-selectins and sLe^x play essential roles in zymosan-induced inflammation. In β4GalT-I–deficient mice, neutrophil recruitment was fully reduced, and ear swelling was partially reduced, suggesting that the selectin ligands on neutrophils were greatly compromised in β4GalT-I–deficient mice.

CHS and DTH responses are commonly used as a model of chronic inflammatory diseases.[32] These responses consist of the initial sensitizing phase and the subsequent elicitation phase. A sensitizing allergen such as TNCB or mBSA applied epidermally is captured by Langerhans cells in the skin. Langerhans cells then migrate to draining lymph nodes and present the allergen to naive T cells in the sensitizing phase. The elicitation phase occurs when epidermal cells encounter the same allergen to which they have been previously exposed. The primed $CD8^+$ Tc1 cells and $CD4^+$ Th1 cells mount CHS and DTH responses, respectively, at the site of challenge and secrete cytokines and chemokines. These cytokines and chemokines recruit neutrophils, monocytes, and lymphocytes to the site of challenge.

CHS and DTH responses were partially, but significantly, suppressed in the β4GalT-I–deficient mice (Figures 7, 8). The β4GalT-I–deficient mice were impaired in neutrophil trafficking to the inflammatory sites in the CHS response (Figure 7B), probably because the amount of P-selectin ligands on neutrophils was reduced (Figure 4A). Therefore, the defect in neutrophil recruitment to the inflammatory sites during the elicitation phase might be the cause of the reduced CHS and DTH responses in the β4GalT-I–deficient mice. The oxazolone-induced CHS response is reduced in E- and P-selectin double-deficient mice, and neutrophil recruitment to the inflammatory sites is reduced during the elicitation phase by the P- or E/P-selectin deficiency.[31,38,42] These reports are consistent with our results. The CHS response induced by 2,4-dinitrofluorobenzene (DNFB) is completely abrogated in Fuc-TIV/VII double-deficient mice.[43] Fuc-TIV/VII double-deficient mice are impaired in L-selectin–dependent naive T-cell trafficking to PLNs and in E- and P-selectin–dependent Th1 and Tc1 T-cell trafficking to inflamed cutaneous sites. These defects result in a reduction of the CHS response in these mice. However, β4GalT-I–deficient mice showed normal lymphocyte homing to PLNs (Figure 5D), suggesting that the cause of the suppression of the CHS response is different between the β4GalT-I–deficient and Fuc-TIV/VII double-deficient mice.

The peripheral leukocytosis and reduced acute and chronic inflammatory responses observed in the β4GalT-I–deficient mice could be well explained by the deficiency of selectin-ligand biosynthesis in these mice. However, the carbohydrate structures of many glycoproteins are considerably changed, such as the shift of the outer chain moieties of the *N*-glycans from type 2 to type 1 chains, in β4GalT-I–deficient mice.[24] We cannot rule out the possibility that other carbohydrate epitopes rather than selectin ligands caused the immunologic abnormalities we observed in the β4GalT-I–deficient mice.

Human congenital disorders of glycosylation and their animal models

A deficiency of glycosyltransferases might be the cause of some human congenital disorders of glycosylation (CDGs). The phenotype of β4GalT-I–deficient mice is similar to that found in patients with leukocyte adhesion deficiency 2 (LAD 2), who exhibit pronounced neutrophilia and have chronic severe periodontitis and mental and growth retardation.[44] E- and P-selectin–deficient mice mimic the human syndrome given that they develop periodontal disease.[45] LAD 2 is caused by selectin ligand deficiency, and a causal gene has been recently identified to encode a putative GDP-fucose transporter, designated CDG-IIc.[46,47]

A human mutation in the *β4GalT-I* gene has been recently identified in an 18-month-old boy with mental retardation, hydrocephalus, myopathy, and blood-clotting defects.[48,49] This is a new type of congenital disorder of glycosylation, designated CDG-IId. Because only a single infant patient has been identified to date and only a few biochemical parameters were analyzed in the patient, it is still unknown whether the human mutation in the *β4GalT-I* gene causes the selectin-ligand deficiency and impaired inflammatory responses we observed in the mouse. In any case, our β4GalT-I–deficient mouse could be an animal model of CDG-IId syndrome. Further analysis of β4GalT-I–deficient mice may be of benefit to patients with CDG-IId and to our understanding of the syndrome.

Acknowledgments

We thank Dr T. Nagata at the Hatano Research Institute, Food and Drug Safety Center for valuable comments for the histologic analysis. We also thank Drs A. Traunecker (Basel Institute for Immunology), Y. Kanakura (Osaka University Graduate School of Medicine), and T. Yoshimoto (Institute for Medical Sciences, University of Tokyo) for human IgM heavy chain, 293T cells, and PE-antirat IgG.

References

1. Springer TA. Traffic signals on endothelium for lymphocyte recirculation and leukocyte emigration. Annu Rev Physiol. 1995;57:827-872.
2. McEver RP, Moore KL, Cummings RD. Leukocyte trafficking mediated by selectin-carbohydrate interactions. J Biol Chem. 1995;270:11025-11028.
3. Lowe JB. Selectin ligands, leukocyte trafficking, and fucosyltransferase genes. Kidney Int. 1997; 51:1418-1426.
4. Mitsuoka C, Sawada-Kasugai M, Ando-Furui K, et al. Identification of a major carbohydrate capping group of the L-selectin ligand on high endothelial venules in human lymph nodes as 6-sulfo sialyl Lewis X. J Biol Chem. 1998;273:11225-11233.
5. Hemmerich S, Rosen SD. Carbohydrate sulfotransferases in lymphocyte homing. Glycobiology. 2000;10:849-856.
6. Leppanen A, Mehta P, Ouyang YB, et al. A novel glycosulfopeptide binds to P-selectin and inhibits leukocyte adhesion to P-selectin. J Biol Chem. 1999;274:24838-24848.
7. Maemura K, Fukuda M. Poly-*N*-acetyllactosaminyl *O*-glycans attached to leukosialin: the presence of sialyl Le(x) structures in *O*-glycans. J Biol Chem. 1992;267:24379-24386.
8. Wilkins PP, McEver RP, Cummings RD. Structures of the *O*-glycans on P-selectin glycoprotein ligand-1 from HL-60 cells. J Biol Chem. 1996; 271:18732-18742.
9. Hiraoka N, Petryniak B, Nakayama J, et al. A novel, high endothelial venule-specific sulfotransferase expresses 6-sulfo sialyl Lewis(x), an L-selectin ligand displayed by CD34. Immunity. 1999;11:79-89.
10. Ju T, Brewer K, D'Souza A, Cummings RD, Canfield WM. Cloning and expression of human core 1 beta1,3-galactosyltransferase. J Biol Chem. 2002;4:178-186.
11. Ellies LG, Tsuboi S, Petryniak B, Lowe JB, Fukuda M, Marth JD. Core 2 oligosaccharide biosynthesis distinguishes between selectin ligands essential for leukocyte homing and inflammation. Immunity. 1998;9:881-890.
12. Yeh JC, Hiraoka N, Petryniak B, et al. Novel sulfated lymphocyte homing receptors and their control by a Core1 extension beta 1,3-*N*-acetylglucosaminyltransferase. Cell. 2001;105:957-969.
13. Maly P, Thall A, Petryniak B, et al. The alpha(1,3) fucosyltransferase Fuc-TVII controls leukocyte trafficking through an essential role in L-, E-, and P-selectin–ligand biosynthesis. Cell. 1996;86:643-653.
14. Homeister JW, Thall AD, Petryniak B, et al. The alpha(1,3)fucosyltransferases FucT-IV and FucT-VII exert collaborative control over selectin-dependent leukocyte recruitment and lymphocyte homing. Immunity. 2001;15:115-126.
15. Solter D, Knowles BB. Monoclonal antibody defining a stage-specific mouse embryonic antigen (SSEA-1). Proc Natl Acad Sci U S A. 1978;75:5565-5569.
16. Hoffman S, Edelman GM. Kinetics of homophilic binding by embryonic and adult forms of the neural cell adhesion molecule. Proc Natl Acad Sci U S A. 1983;80:5762-5766.
17. Kellhauer G, Falssner A, Schachner M. Differential inhibition of neurone-neurone, neurone-astrocyte and astrocyte-astrocyte adhesion by L1, L2, and N-CAM antibodies. Nature. 1985;316:728-730.
18. Yamamoto S, Oka S, Inoue M, et al. Mice deficient in nervous system-specific carbohydrate epitope HNK-1 exhibit impaired synaptic plasticity and spatial learning. J Biol Chem. 2002;277: 27227-27231.
19. Eckhardt M, Bukalo O, Chazal G, et al. Mice deficient in the polysialyltransferase ST8SiaIV/PST-1 allow discrimination of the roles of neural cell adhesion molecule protein and polysialic acid in neural development and synaptic plasticity. J Neurosci. 2000;20:5234-5244.
20. Asano M, Furukawa K, Kido M, et al. Growth retardation and early death of beta-1,4–galactosyltransferase knockout mice with augmented proliferation and abnormal differentiation of epithelial cells. EMBO J. 1997;16:1850-1857.
21. Lu Q, Hasty P, Shur BD. Targeted mutation in beta1,4-galactosyltransferase leads to pituitary insufficiency and neonatal lethality. Dev Biol. 1997;181:257-267.
22. Kido M, Asano M, Iwakura Y, Ichinose M, Miki K, Furukawa K. Presence of polysialic acid and HNK-1 carbohydrate on brain glycoproteins from beta-1,4-galactosyltransferase-knockout mice. Biochem Biophys Res Commun. 1998;245:860-864.
23. Hennet T. The galactosyltransferase family. Cell Mol Life Sci. 2002;59:1081-1095.
24. Kotani N, Asano M, Iwakura Y, Takasaki S. Knockout of mouse beta1,4-galactosyltransferase-1 gene results in a dramatic shift of outer chain moieties of *N*-glycans from type 2 to type 1 chains in hepatic membrane and plasma glycoproteins. Biochem J. 2001;357:827-834.
25. Kotani N, Asano M, Iwakura Y, Takasaki S. Impaired galactosylation of core 2 *O*-glycans in erythrocytes of beta1,4-galactosyltransferase knockout mice. Biochem Biophys Res Commun. 1999;260:94-98.
26. Kotani N, Takasaki S. Analysis of *O*-linked oligosaccharide alditols by high-pH anion-exchange chromatography with pulsed amperometric detection. Anal Biochem. 1997;252:40-47.
27. Homeister JW, Zhang M, Frenette PS, et al. Overlapping functions of E- and P-selectin in neutrophil recruitment during acute inflammation. Blood. 1998;92:2345-2352.
28. Higgins LM, McDonald SA, Whittle N, Crockett N, Shields JG, MacDonald TT. Regulation of T cell activation in vitro and in vivo by targeting the OX40-OX40 ligand interaction: amelioration of ongoing inflammatory bowel disease with an OX40-IgG fusion protein, but not with an OX40 ligand-IgG fusion protein. J Immunol. 1999;162:486-493.
29. Yang J, Hirata T, Croce K, et al. Targeted gene disruption demonstrates that P-selectin glycoprotein ligand 1 (PSGL-1) is required for P-selectin–mediated but not E-selectin–mediated neutrophil rolling and migration. J Exp Med. 1999;190:1769-1782.
30. Frenette PS, Mayadas TN, Rayburn H, Hynes RO, Wagner DD. Susceptibility to infection and altered hematopoiesis in mice deficient in both P- and E-selectins. Cell. 1996;84:563-574.
31. Staite ND, Justen JM, Sly LM, Beaudet AL, Bullard DC. Inhibition of delayed-type contact hypersensitivity in mice deficient in both E-selectin and P-selectin. Blood. 1996;88:2973-2979.
32. Grabbe S, Schwarz T. Immunoregulatory mechanisms involved in elicitation of allergic contact hypersensitivity. Immunol Today. 1998;19:37-44.
33. Furukawa K, Sato T. Beta-1,4-galactosylation of *N*-glycans is a complex process. Biochim Biophys Acta. 1999;1473:54-66.
34. Ujita M, McAuliffe J, Schwientek T, et al. Synthesis of poly-*N*-acetyl lactosamine in core 2 branched *O*-glycans: the requirement of novel beta-1,4-galactosyltransferase IV and beta-1,3-*N*-acetylglucosaminyltransferase. J Biol Chem. 1998;273:34843-34849.
35. Ujita M, Misra AK, McAuliffe J, Hindsgaul O, Fukuda M. Poly-*N*-acetyl lactosamine extension in *N*-glycans and core 2- and core 4-branched *O*-glycans is differentially controlled by i-extension enzyme and different members of the beta 1,4-galactosyltransferase gene family. J Biol Chem. 2000;275:15868-15875.
36. Seko A, Dohmae N, Takio K, Yamashita K. β 1,4-Galactosyltransferase (β 4GalT)-IV is specific for GlcNAc 6-*O*-sulfate: β 4GalT-IV acts on keratan sulfate-related glycans and a precursor glycan of 6-sulfosialyl-Lewis x. J Biol Chem. 2003;278: 9150-9158.
37. Mayadas TN, Johnson RC, Rayburn H, Hynes RO, Wagner DD. Leukocyte rolling and extravasation are severely compromised in P-selectin–deficient mice. Cell. 1993;74:541-554.
38. Labow MA, Norton CR, Rumberger JM, et al. Characterization of E-selectin–deficient mice: demonstration of overlapping function of the endothelial selectins. Immunity. 1994;1:709-720.
39. Arbones ML, Ord DC, Ley K, et al. Lymphocyte homing and leukocyte rolling and migration are impaired in L-selectin–deficient mice. Immunity. 1994;1:247-260.
40. Bullard DC, Kunkel EJ, Kubo H, et al. Infectious susceptibility and severe deficiency of leukocyte rolling and recruitment in E-selectin and P-selectin double mutant mice. J Exp Med. 1996;183: 2329-2336.
41. Johnson RC, Mayadas TN, Frenette PS, et al. Blood cell dynamics in P-selectin–deficient mice. Blood. 1995;86:1106-1114.
42. Subramaniam M, Saffaripour S, Watson SR, Mayadas TN, Hynes RO, Wagner DD. Reduced recruitment of inflammatory cells in a contact hypersensitivity response in P-selectin–deficient mice. J Exp Med. 1995;181:2277-2282.
43. Smithson G, Rogers CE, Smith PL, et al. Fuc-TVII is required for T helper 1 and T cytotoxic 1 lymphocyte selectin ligand expression and recruitment in inflammation, and together with Fuc-TIV regulates naive T cell trafficking to lymph nodes. J Exp Med. 2001;194:601-614.
44. Etzioni A, Tonetti M. Leukocyte adhesion deficiency II: from A to almost Z. Immunol Rev. 2000;178:138-147.
45. Niederman R, Westernoff T, Lee C, et al. Infection-mediated early-onset periodontal disease in P/E-selectin–deficient mice. J Clin Periodontol. 2001;28:569-575.
46. Luhn K, Wild MK, Eckhardt M, Gerardy-Schahn R, Vestweber D. The gene defective in leukocyte adhesion deficiency II encodes a putative GDP-fucose transporter. Nat Genet. 2001;28:69-72.
47. Lubke T, Marquardt T, Etzioni A, Hartmann E, von Figura K, Korner C. Complementation cloning identifies CDG-IIc, a new type of congenital disorders of glycosylation, as a GDP-fucose transporter deficiency. Nat Genet. 2001;28:73-76.
48. Hansske B, Thiel C, Lubke T, et al. Deficiency of UDP-galactose:*N*-acetylglucosamine beta-1,4-galactosyltransferase I causes the congenital disorder of glycosylation type IId. J Clin Invest. 2002;109:725-733.
49. Peters V, Penzien JM, Reiter G, et al. Congenital disorder of glycosylation IId (CDG-IId): a new entity: clinical presentation with Dandy-Walker malformation and myopathy. Neuropediatrics. 2002; 33:27-32.

IL-17 production from activated T cells is required for the spontaneous development of destructive arthritis in mice deficient in IL-1 receptor antagonist

Susumu Nakae*, Shinobu Saijo*, Reiko Horai*, Katsuko Sudo*, Shigeo Mori†, and Yoichiro Iwakura*‡

*Center for Experimental Medicine and †Department of Cancer Biology, Institute of Medical Science, University of Tokyo, 4-6-1 Shirokanedai, Minato-ku, Tokyo 108-8639, Japan

Edited by Charles A. Dinarello, University of Colorado Health Sciences Center, Denver, CO, and approved March 24, 2003 (received for review October 4, 2002)

IL-17 is a T cell-derived, proinflammatory cytokine that is suspected to be involved in the development of various inflammatory diseases. Although there are elevated levels of IL-17 in synovial fluid of patients with rheumatoid arthritis, the pathogenic role of IL-17 in the development of rheumatoid arthritis remains to be elucidated. In this report, the effects of IL-17 deficiency were examined in IL-1 receptor antagonist-deficient (IL-1Ra$^{-/-}$) mice that spontaneously develop an inflammatory and destructive arthritis due to unopposed excess IL-1 signaling. IL-17 expression is greatly enhanced in IL-1Ra$^{-/-}$ mice, suggesting that IL-17 activity is involved in the pathogenesis of arthritis in these mice. Indeed, the spontaneous development of arthritis did not occur in IL-1Ra$^{-/-}$ mice also deficient in IL-17. The proliferative response of ovalbumin-specific T cells from DO11.10 mice against ovalbumin cocultured with antigen-presenting cells from either IL-1Ra$^{-/-}$ mice or wild-type mice was reduced by IL-17 deficiency, indicating insufficient T cell activation. Cross-linking OX40, a cosignaling molecule on CD4$^+$ T cells that plays an important role in T cell antigen-presenting cell interaction, with anti-OX40 Ab accelerated the production of IL-17 induced by CD3 stimulation. Because OX40 is induced by IL-1 signaling, IL-17 induction is likely to be downstream of IL-1 through activation of OX40. These observations suggest that IL-17 plays a crucial role in T cell activation, downstream of IL-1, causing the development of autoimmune arthritis.

IL-17, a T cell-derived proinflammatory cytokine, is produced by TCRα/β^+CD4$^-$CD8$^-$ thymocytes, as well as by activated CD4$^+$ and CD4$^+$CD45RO$^+$ memory T cells (1). IL-17 has pleiotropic activities including the induction of proinflamatory cytokines such as tumor necrosis factor α, IL-1β, and IL-6, and chemokines like IL-8 and monocyte chemoattractant protein 1 on various cell types (2, 3). In addition, IL-17 is involved in the induction of inducible nitric oxide synthase and cyclooxygenase 2 in chondrocytes (4), induction of prostaglandin E2-mediated osteoclast differentiation factor expression in osteoblasts (5), up-regulation of intracellular adhesion molecule 1 and HLA-DR expression in kerationocytes (6), promotion of stem cell factor- and granulocyte-colony stimulating factor-mediated granulopoiesis (7), promotion of tumor rejection by natural killer cell activation (8), and enhancement of allorejection via promotion of dendritic cell maturation (9).

IL-17 has been suggested to be involved in the development of rheumatoid arthritis (RA), because IL-17 is found in the synovial fluid of patients with RA (10) and is produced by T cell clones established from patients with RA (11). Actually, the incidence of arthritis can be partially reduced by the administration of an extracellular domain of IL-17R and Fc fusion protein (IL-17R:Fc), which inhibits IL-17-IL-17R binding in the elicitation phase during collagen-induced arthritis (CIA) (12). The precise role for IL-17 in the pathogenesis of RA, however, still remains to be elucidated.

IL-1 receptor antagonist (IL-1Ra) is an endogenous inhibitor of IL-1 and is believed to regulate IL-1 activity. Polyarthritis spontaneously develops in IL-1Ra$^{-/-}$ mice on the BALB/c background starting at 5 weeks of age, and by 12 weeks of age almost all mice are affected (13). Histopathology of the lesions closely resembles RA in humans, with marked synovial and periarticular inflammation and articular erosion caused by invasion of granulation tissue (13). High levels of auto-Abs against Ig, type II collagen (IIC), and double-stranded DNA are detectable in serum. When IL-1Ra$^{-/-}$ mice are crossed to *scid/scid* mice, the development of arthritis is completely suppressed (R.H., A. Nakajima, and Y.I., unpublished data). Furthermore, when T cells from IL-1Ra$^{-/-}$ mice are transferred to *nu/nu* mice, these mice develop arthritis (ref. 14; R.H. and Y.I., unpublished data). Thus, in this model, excess IL-1 signaling due to a deficiency in the IL-1Ra gene product causes T cell-mediated autoimmunity, resulting in joint-specific inflammation and bone destruction.

In this study, using IL-17$^{-/-}$ mice, we assessed the role of IL-17 in the development of arthritis in IL-1Ra$^{-/-}$ mouse models. We show that IL-17 production by T cells is greatly enhanced in IL-1Ra$^{-/-}$ mice, and IL-17 deficiency completely blocks the development of arthritis of this model. Furthermore, we demonstrate that cross-linking of OX40 on T cells enhances IL-17 production, suggesting that IL-1 enhances IL-17 production through OX40 induction.

Materials and Methods

Mice. IL-17$^{-/-}$ and IL-1Ra$^{-/-}$ mice were generated as described (15, 16). IL-17-deficient IL-1Ra$^{-/-}$ mice were produced by crossing IL-17$^{-/-}$ mice, backcrossed three generations to BALB/cA mice, and then to IL-1Ra$^{-/-}$ mice on the BALB/cA background (N8). DO11.10 transgenic mice were kindly supplied by D. Y. Loh (17). These mice were kept under specific pathogen-free conditions in an environmentally controlled clean room in the Center for Experimental Medicine at the Institute of Medical Science, University of Tokyo. The experiments were conducted according to the institutional ethical guidelines for animal experiments and the safety guidelines for gene manipulation experiments.

Clinical Assessment of Arthritis. Development of arthritis by macroscopic evaluation was determined as described (13). The histological score was evaluated independently by two individuals blind to the genotypes of the mice.

T Cell Culture. To measure IL-17 production from lymph node (LN) cells, axillary, inguinal, and brachial LN cells were harvested from wild-type or IL-1Ra$^{-/-}$ mice. LN cells (2×10^5 cells

This paper was submitted directly (Track II) to the PNAS office.

Abbreviations: IL-1Ra, IL-1 receptor antagonist; RA, rheumatoid arthritis; CIA, collagen-induced arthritis; LN, lymph node; APC, antigen-presenting cell; IIC, type II collagen.

‡To whom correspondence should be addressed. E-mail: iwakura@ims.u-tokyo.ac.jp.

www.pnas.org/cgi/doi/10.1073/pnas.1035999100

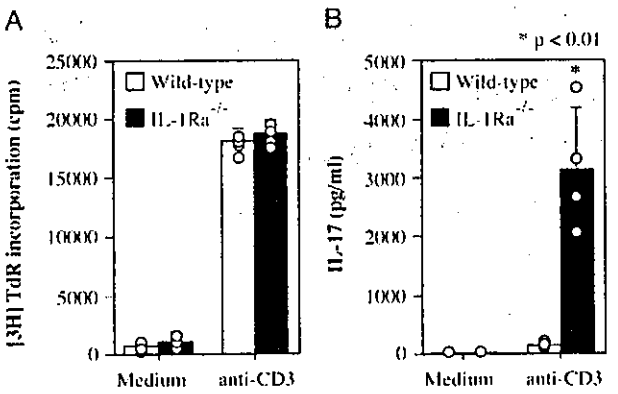

Fig. 1. IL-17 production is markedly enhanced in T cells from IL-1Ra$^{-/-}$ mice. LN cells from wild-type and IL-1Ra$^{-/-}$ mice were cultured in the absence or presence of 1 μg/ml anti-CD3 mAb for 48 h. (*A*) Proliferative response was measured by [^{3}H]thymidine incorporation. (*B*) IL-17 levels in the supernatants of *A* were determined by ELISA. Each circle represents an individual mouse, and an average and SD are shown. These results were reproducible in two independent experiments. The Student's *t* test was used for statistical evaluation of the results.

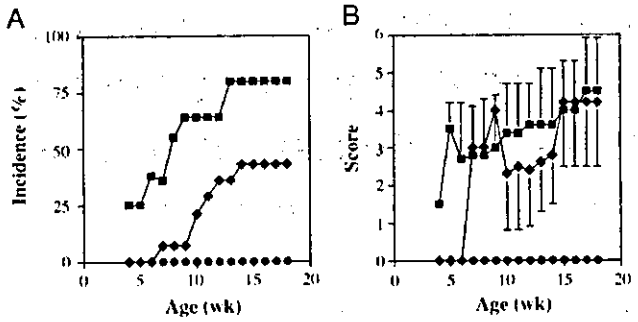

Fig. 2. Development of arthritis in IL-1Ra$^{-/-}$ mice is completely suppressed by a deficiency of IL-17. (*A*) Incidence of arthritis that developed in IL-1Ra$^{-/-}$ mice on the BALB/c background. The incidences were compared among IL-17$^{-/-}$, IL-17$^{+/-}$, and IL-17$^{+/+}$ mice. (*B*) Severity score of the mice. Average scores of the affected mice are shown and bars represent the SD. Squares, IL-17$^{+/+}$ × IL-1Ra$^{-/-}$ (n = 10); diamonds, IL-17$^{+/-}$ × IL-1Ra$^{-/-}$ mice (n = 14); circles, IL-17$^{-/-}$ × IL-1Ra$^{-/-}$ mice (n = 10).

per well in a 96-well flat-bottom plate) were cultured in the absence or presence of 1 μg/ml anti-CD3 mAb (145-2C11; BD Pharmingen), after which IL-17 levels were measured in the culture medium.

To purify CD4$^+$ T cells, spleen cell suspensions were passed through a nylon wool column. Then, the flow-through fraction was incubated with anti-CD8, anti-B220, anti-Mac-1, anti-Ter119, and anti-DX5 magnetic beads (Miltenyi Biotec, Bergisch Gladbach, Germany) and passed through a magnetic cell sorting column (Miltenyi Biotec), and the negative fraction was collected (CD4$^+$ T cells >95%). CD4$^+$ T cells (2×10^5 cells per well in a 96-well flat-bottom plate) were cultured in a plate coated with an anti-CD3 mAb, a mixture of anti-CD3 mAb (0.5 μg/ml) plus recombinant IL-1α (PeproTech, Rocky Hill, NJ), or a mixture of anti-CD3 mAb (1 μg/ml) plus anti-OX40 mAb (OX86; BD Pharmingen). In the anti-CD3 plus anti-OX40 stimulation, data are shown from the time point of maximal response in IL-17 production (96 h). In the primary T cell response assay, CD4$^+$ T cells (2.5×10^5 cells) from DO11.10 transgenic mice were cultured with antigen-presenting cells (APCs) as B220$^-$Thy1.2$^-$ splenic adherent cells (5×10^3 cells) in the absence or presence of 0.1 μM ovalbumin peptide for 3 days as described (18).

For collagen-specific LN cell culture, mice were immunized intradermally at the base of the tail with 200 μg of bovine IIC (Cosmobio, Tokyo) in 0.02 M Tris·HCl/0.15 M NaCl with Freund's complete adjuvant (Difco) and killed 7 days later. LN cells (1×10^6 cells per ml; inguinal, axillary, brachial, and submaxillary) were cultured in the absence or presence of 20 μg/ml IIC for 24 h (for CD40L expression) or 72 h (for OX40 expression). Then, fluorescence-activated cell sorter analysis was carried out as described (19).

Detection of IL-17 by ELISA. IL-17 levels were measured by ELISA as described (15). Monoclonal rat anti-mouse IL-17 and polyclonal biotinylated goat anti-mouse IL-17 Abs (DAKO) were used as capture and detection Abs, respectively. Horseradish peroxidase–avidin was obtained from PharMingen and TMB substrate (3.5′–5.5′ tetramethylbenzidine and hydrogen peroxide) was purchased from DAKO. Recombinant IL-17 as a standard reagent was obtained from Sigma.

Fluorescence-Activated Cell Sorter Analysis. CD40L expression on CD4$^+$ T cells was analyzed as described (20). Briefly, to determine the effect of IL-17 on CD40L expression, purified CD4$^+$ T cells from IIC-immunized mice on 12-well plates (1×10^6 cells per well) were stimulated with plate-coated CD3 mAb with or without rIL-17 in the presence of 1 μg of biotinylated anti-mouse CD40L mAb (MR1; BD Pharmingen) or biotinylated hamster IgG (BD Pharmingen) as an isotype-matched control Ab for 24 h. OX40 expression on CD4$^+$ T cells was examined as described (18). FITC-anti-mouse CD4 mAb (RM4–5) and phycoerythrin (PE)–streptavidin were purchased from BD Pharmingen. PE-anti-mouse OX40 mAb (OX86) was obtained from Immunotech (Luminy, France).

Immunohistochemistry. To detect OX40 expression on synovial tissue of IL-1Ra$^{-/-}$ mice, immunohistochemical analysis was performed as described (21). In brief, mouse limbs were fixed in

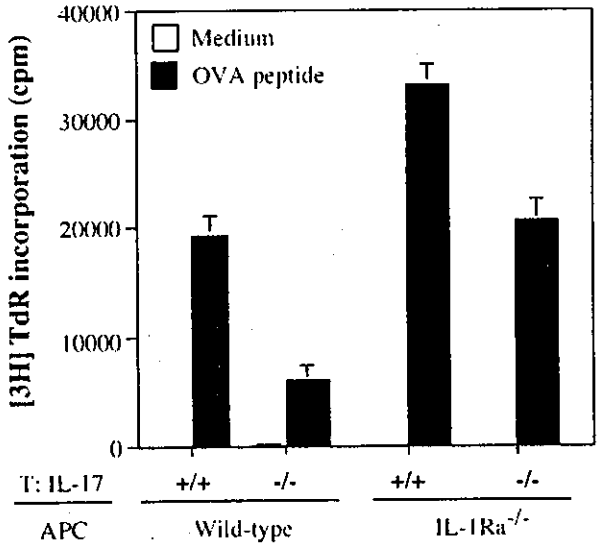

Fig. 3. IL-17 is required for antigen-specific T cell priming. Proliferative responses of DO11.10 T cells against the ovalbumin 323–339 peptide in the presence of APCs from wild-type or IL-1Ra$^{-/-}$ mice were assessed by measuring the incorporation of [^{3}H]thymidine after 3 days of culture. Effects of IL-17 deficiency were evaluated by using IL-17$^{-/-}$ DO11.10 T cells and IL-1Ra$^{-/-}$ APCs. Data shows an average ± SD of three wells. These results were reproducible in two independent experiments.

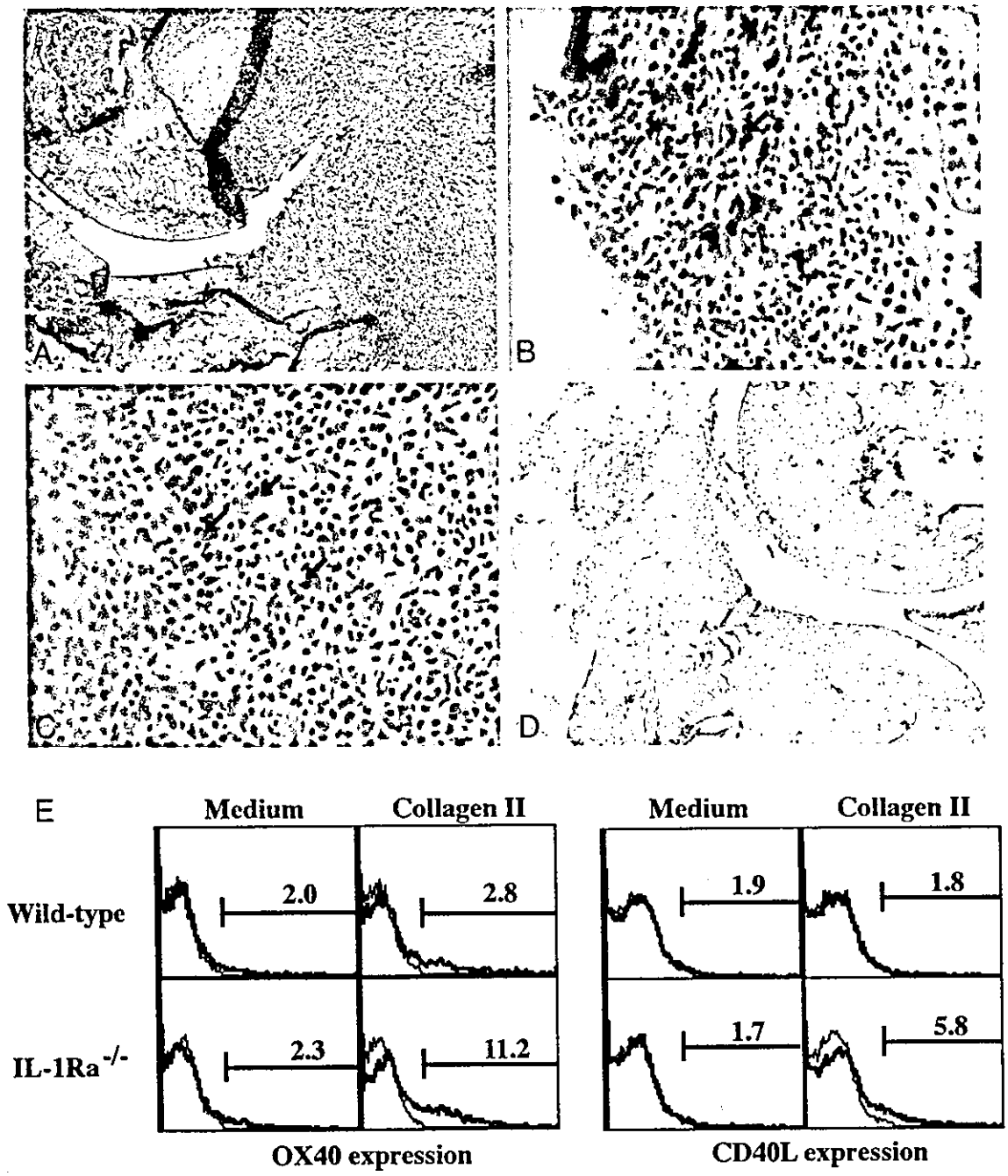

Fig. 4. Enhanced OX40 and CD40L expression on T cells in IL-1Ra$^{-/-}$ mice. CD4$^+$ and OX40$^+$ cell infiltration was observed in synovial tissues of IL-1Ra$^{-/-}$ mice (*A–C*) but not in wild-type mice (*D*). Both OX40 and CD40L expression on CD4$^+$ T cells was enhanced in IL-1Ra$^{-/-}$ mice compared with wild-type mice after immunization with IIC (*E*). (*A*) Synovial tissues of IL-1Ra$^{-/-}$ mice; hematoxylin/eosin (H&E) staining (magnification, ×25). (*B*) Synovial tissues of IL-1Ra$^{-/-}$ mice stained with anti-CD4 mAb (magnification, ×100). Arrow shows positive cells. (*C*) Synovial tissues of IL-1Ra$^{-/-}$ mice stained with anti-OX40 mAb (magnification, ×100). Arrows show positive cells. (*D*) Synovial tissues of wild-type mice; H&E staining (magnification, ×25). (*E*) Seven days after immunization with IIC, LN cells were cultured in the absence or presence of 20 μg/ml IIC for 24 (CD40L expression) or 72 h (OX40 expression). Then, CD40L and OX40 expression in CD4$^+$ population was analyzed by flow cytometry. Shaded area shows an isotype-matched control Ig staining.

PLP solution (0.02 g/ml paraformaldehyde/0.015 M L-lysine monohydochloride, pH 7.4/0.01 M sodium perchlorate) for 6 h at 4°C. After fixing, limbs were decalcified in EDTA–glycerol solution (0.35 M dipotassium dihydrogen ethylenediaminetetraacetate/15% glycerol) for 10 days. Then, samples were embedded in OCT compound and prepared slices.

Results and Discussion

To investigate the role of IL-17 in the development of arthritis in IL-1Ra$^{-/-}$ mice, we examined IL-17 production in T cells from these mice. LN cells containing both T cells and APCs from arthritic IL-1Ra$^{-/-}$ mice were stimulated with anti-CD3 mAb,

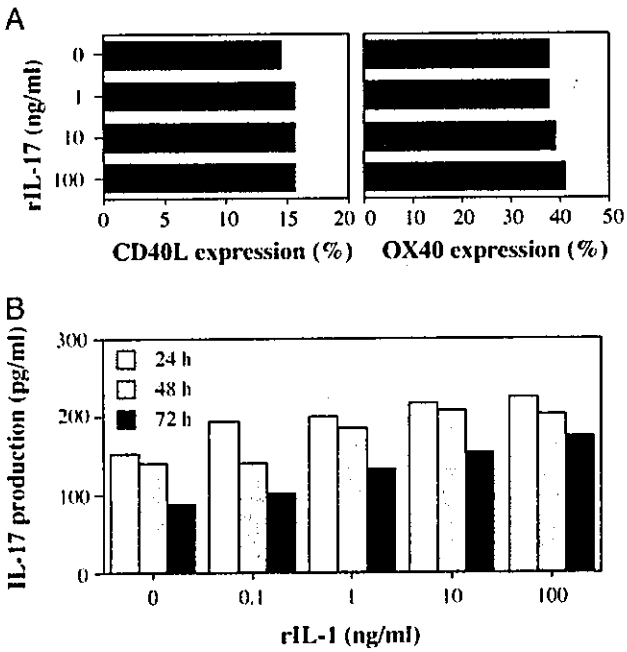

Fig. 5. IL-1 could not directly induce IL-17 in CD4+ T cells. (*A*) IL-17 could not induce CD40L and OX40 expression on CD4+ T cells. Splenic CD4+ T cells from wild-type mice were stimulated with plate-coated anti-mouse CD3 mAb (1 μg/ml) with or without rIL-17 for 24 (for CD40L expression) and 72 h (for OX40 expression). These results were reproducible in two independent experiments. (*B*) Splenic CD4+ T cells from wild-type mice were stimulated with or without rIL-1α together with plate-coated anti-mouse CD3 mAb for 24, 48, and 72 h. Then, IL-17 levels in culture supernatants were determined by ELISA. Data show a pooled supernatant from three wells. These results were reproducible in two independent experiments.

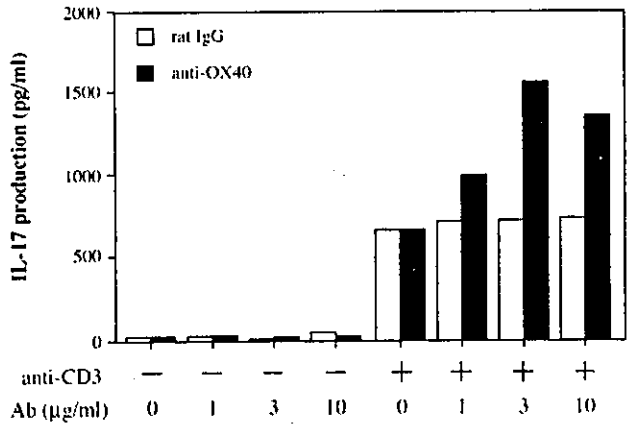

Fig. 6. Cross-linking of OX40 on CD4+ T cells promotes IL-17 production. Cross-linking of OX40 could promote IL-17 production by CD4+ T cells. Splenic CD4+ T cells from wild-type mice were stimulated with plate-coated anti-mouse CD3 mAb (1 μg/ml) plus varying amounts of plate-coated anti-OX40 mAb or isotype control rat IgG for 96 h. Then, IL-17 levels in culture supernatants were determined by ELISA. Data show a pooled supernatant from three wells. These results were reproducible in three independent experiments.

and T cell proliferation and IL-17 production were measured. Proliferative responses of IL-1Ra$^{-/-}$ T cells were comparable to those of wild-type T cells (Fig. 1*A*), indicating that the T cell antigen receptor signaling pathway underlying proliferative responses was normal in these mutant mice. In contrast, IL-17 production by IL-1Ra$^{-/-}$ T cells was markedly enhanced relative to wild-type T cells (Fig. 1*B*). Thus, excess IL-1 signaling, caused by a deficiency of IL-1Ra, induces IL-17 production, suggesting that IL-17 may be involved in the development of arthritis in IL-1Ra$^{-/-}$ mice.

To verify this possibility, we assessed the effect of IL-17 deficiency on the development of arthritis in IL-1Ra$^{-/-}$ mice. IL-17$^{-/-}$ and IL-1Ra$^{-/-}$ double-deficient mice were generated by intercrossing single mutant mice, and the incidence of arthritis in IL-17$^{-/-}$ × IL-1Ra$^{-/-}$ mice was investigated. We found that the development of arthritis in IL-17$^{-/-}$ × IL-1Ra$^{-/-}$ mice was completely suppressed, as shown in Fig. 2*A*. The incidence of arthritis in IL-17$^{+/-}$ × IL-1Ra$^{-/-}$ mice was also significantly lower than that in IL-17$^{+/+}$ × IL-1Ra$^{-/-}$ mice, indicating a gene dosage effect of IL-17. These results indicate that IL-17 is involved in the development of arthritis caused by excess IL-1 signaling.

Interestingly, the severity score of arthritis in IL-17 heterozygous mice was similar to that of wild-type mice, even though the incidence was significantly suppressed (Fig. 2*B*). These results suggest that IL-17 plays a role in the sensitization phase rather than in the elicitation phase. To verify this possibility, we examined the effect of IL-17 on antigen-specific T cell activation by using DO11.10 mice that carry an ovalbumin (OVA)-specific T cell receptor transgene. The proliferative response of CD4+ T cells from IL-17$^{-/-}$ DO11.10 transgenic mice cocultured with IL-1Ra$^{-/-}$ APCs directed against OVA was decreased to the level of DO11.10 CD4+ T cells cocultured with wild-type APCs. In contrast, a greater proliferative response was detected in IL-17$^{+/+}$ DO11.10 T cells cocultured with IL-1Ra$^{-/-}$ APCs (Fig. 3). These results clearly indicate that IL-17 is required for activating naive T cells in an antigen-specific manner, and that the activation of T cells by IL-1 is mediated via IL-17.

We recently showed that IL-1 produced by APCs induced CD40L and OX40 expression on CD4+ T cells (18). CD40L and OX40 act as costimulatory molecules in T cell–APC interaction, and these molecules are suggested to be involved in the development of arthritis (22–25). Consistent with this notion, the blockade of CD40L–CD40 or OX40–OX40L interaction suppressed the development of arthritis in IL-1Ra$^{-/-}$ mice (ref. 14; R.H. and Y.I., unpublished data). Actually, OX40+ cells were detected in the follicular structure resembling secondary lymphoid follicles in the synovial tissue (Fig. 4 *A* and *C*), where CD4+ cells were accumulated (Fig. 4*B*). Similar follicular structures are formed in synovial tissues of patients with RA (26). On the other hand, CD40L expression could not be detected histologically in synovial tissues of IL-1Ra$^{-/-}$ mice. With regard to this, it is known that CD40L expression on cell surface is very low because of down-modulation of the expression by CD40 cross-linking (27, 28). Then, we examined CD40L and OX40 expression on T cells from IL-1Ra$^{-/-}$ mice after stimulation with IIC, which was known as one of autoantigens in the synovial tissues (13). As shown in Fig. 4*E*, the expression of CD40L and OX40 on CD4+ T cells in IL-1Ra$^{-/-}$ mice was augmented compared with that in wild-type mice. These observations suggest that CD40L and OX40 expression on CD4+ T cells in synovial tissues is enhanced in IL-1Ra$^{-/-}$ mice. This enhancement, however, was not induced by IL-17, because treatment with rIL-17 did not induce CD40L or OX40 expression on CD4+ T cells (Fig. 5*A*).

We next analyzed the mechanism of IL-17 induction. Because the previous results indicate that IL-17 functions downstream of IL-1, we examined the possibility that IL-1 directly induces IL-17 production in T cells. When purified CD4+ T cells from LN cells were treated with varying concentrations of IL-1, together with stimulation by plate-coated anti-CD3 mAb (0.5 μg/ml) for 24, 48, and 72 h, essentially no stimulation of IL-17 production was

IMMUNOLOGY

observed (Fig. 5*B*). Thus, overproduction of IL-17 in IL-1Ra$^{-/-}$ LN cells is not a result of direct effects of IL-1 on CD4$^+$ T cells.

We next examined the possibility that OX40 signaling might induce IL-17 production, because OX40 expression on T cells is augmented in IL-1Ra$^{-/-}$ mice. As shown in Fig. 6, IL-17 production in plate-coated anti-CD3 mAb-stimulated CD4$^+$ T cells was enhanced by stimulation with plate-coated anti-OX40 mAb. High concentrations (10–100 μg/ml) of anti-OX40 mAb, however, inhibited IL-17 production and T cell proliferation (Fig. 6; data not shown). IL-17 production was not observed with anti-OX40 mAb alone, without anti-CD3 mAb stimulation. These results indicate that OX40 signaling enhances IL-17 production induced by T cell antigen receptor stimulation in CD4$^+$ T cells.

In this report, we have shown that IL-17 production is enhanced by excess IL-1 signaling through activation of OX40 in IL-1Ra$^{-/-}$ mice, resulting in the development of autoimmunity and arthritis. It was reported that systemic or local overproduction of IL-17 with an adenoviral vector accelerated the development of CIA, and inhibition of IL-17 signaling by an IL-17R:Fc fusion protein suppressed the development of CIA in mice (12), indicating an important role for IL-17 in the development of CIA. Moreover, this aggravated CIA could not be suppressed by administration of an anti-IL-1α/β Ab and IL-17-induced exaggeration of bacterial cell wall-induced arthritis was not diminished in IL-1$\beta^{-/-}$ mice, suggesting an IL-1-independent role of IL-17 (12). These observations are consistent with our notion that IL-17 acts downstream of IL-1.

Because IL-17 is produced by activated T cells and can induce various proinflammatory cytokines, chemokines, and cell adhesion molecules (2, 3, 6), it is implied that this cytokine plays an important role in the development of inflammation at the elicitation phase. In this report, however, we have shown that IL-17 plays a crucial role in the activation of T cells at the sensitization phase in the development of arthritis. With regard to this, Yao *et al.* (29) reported that T cell proliferation and IL-2 production induced by phytohemagglutinin, Con A, and anti-T cell antigen receptor mAb were inhibited by soluble IL-17R, indicating that IL-17 is involved in T cell activation. We also observed that T cell sensitization is impaired in IL-17$^{-/-}$ mice after induction of contact hypersensitivity, delayed-type hypersensitivity, and airway hypersensitivity responses (15). The molecular mechanisms by which naive T cells are activated by IL-17, however, remain to be elucidated.

We have shown that auto-Ab levels in sera are elevated in IL-1Ra$^{-/-}$ mice (13). The levels of auto-Abs against IgG (rheumatoid factor) in sera of IL-17$^{-/-}$ × IL-1Ra$^{-/-}$ mice were significantly reduced compared with that of IL-17$^{+/+}$ × IL-1Ra$^{-/-}$ mice [0.111 ± 0.022 (n = 6) vs. 0.152 ± 0.068 (n = 10), P = 0.05], which was consistent with our observation that IL-17 was involved in Ab production (15). This reduction of auto-Ab production in IL-17$^{-/-}$ × IL-1Ra$^{-/-}$ mice, however, may not be the major reason for the suppression of the development of arthritis, because IL-1Ra$^{-/-}$ mouse serum transfer could not induce arthritis in wild-type mice (R.H. and Y.I., data not shown).

Taken together, we have demonstrated that a cascade of IL-1 signaling leads to autoimmunity and arthritis in IL-1Ra$^{-/-}$ mice. Excess IL-1 signaling caused by IL-1Ra deficiency induces excess OX40 expression on T cells, and then, OX40 signaling induces overproduction of IL-17 from CD4$^+$ T cells, leading to the development of autoimmunity and arthritis. These findings may provide a cue for development of novel therapeutics to treat autoimmune inflammatory diseases.

We thank all of the members of the laboratory for animal care. This work was supported by grants from the Ministry of Education, Science, Sports, and Culture of Japan and the Ministry of Health and Welfare of Japan.

1. Yao, Z., Painter, S. L., Fanslow, W. C., Ulrich, D., Macduff, B. M., Spriggs, M. K. & Armitage, R. J. (1995) *J. Immunol.* **155**, 5483–5486.
2. Fossiez, F., Banchereau, J., Murray, R., Van Kooten, C., Garrone, P. & Lebecque, S. (1998) *Int. Rev. Immunol.* **16**, 541–551.
3. Jovanovic, D. V., Di Battista, J. A., Martel-Pelletier, J., Jolicoeur, F. C., He, Y., Zhang, M., Mineau, F. & Pelletier, J. P. (1998) *J. Immunol.* **160**, 3513–3521.
4. Shalom-Barak, T., Quach, J. & Lotz, M. (1998) *J. Biol. Chem.* **273**, 27467–27473.
5. Kotake, S., Udagawa, N., Takahashi, N., Matsuzaki, K., Itoh, K., Ishiyama, S., Saito, S., Inoue, K., Kamatani, N., Gillespie, M. T., *et al.* (1999) *J. Clin. Invest.* **103**, 1345–1352.
6. Albanesi, C., Scarponi, C., Cavani, A., Federici, M., Nasorri, F. & Girolomoni, G. (2000) *J. Invest. Dermatol.* **115**, 81–87.
7. Schwarzenberger, P., Huang, W., Ye, P., Oliver, P., Manuel, M., Zhang, Z., Bagby, G., Nelson, S. & Kolls, J. K. (2000) *J. Immunol.* **164**, 4783–4789.
8. Hirahara, N., Nio, Y., Sasaki, S., Takamura, M., Iguchi, C., Dong, M., Yamasawa, K., Itakura, M. & Tamura, K. (2000) *Anticancer Res.* **20**, 3137–3142.
9. Antonysamy, M. A., Fanslow, W. C., Fu, F., Li, W., Qian, S., Troutt, A. B. & Thomson, A. W. (1999) *J. Immunol.* **162**, 577–584.
10. Ziolkowska, M., Koc, A., Luszczykiewicz, G., Ksiezopolska-Pietrzak, K., Klimczak, E., Chwalinska-Sadowska, H. & Maslinski, W. (2000) *J. Immunol.* **164**, 2832–2838.
11. Aarvak, T., Chabaud, M., Miossec, P. & Natvig, J. B. (1999) *J. Immunol.* **162**, 1246–1251.
12. Lubberts, E., Joosten, L. A., Oppers, B., van den Bersselaar, L., Coenen-de Roo, C. J., Kolls, J. K., Schwarzenberger, P., van de Loo, F. A. & van den Berg, W. B. (2001) *J. Immunol.* **167**, 1004–1013.
13. Horai, R., Saijo, S., Tanioka, H., Nakae, S., Sudo, K., Okahara, A., Ikuse, T., Asano, M. & Iwakura, Y. (2000) *J. Exp. Med.* **191**, 313–320.
14. Iwakura, Y. (2002) *Cytokine Growth Factor Rev.* **13**, 341–355.
15. Nakae, S., Komiyama, Y., Nambu, A., Sudo, K., Iwase, M., Homma, I., Sekikawa, K., Asano, M. & Iwakura, Y. (2002) *Immunity* **17**, 375–387.
16. Horai, R., Asano, M., Sudo, K., Kanuka, H., Suzuki, M., Nishihara, M., Takahashi, M. & Iwakura, Y. (1998) *J. Exp. Med.* **187**, 1463–1475.
17. Murphy, K. M., Heimberger, A. B. & Loh, D. Y. (1990) *Science* **250**, 1720–1723.
18. Nakae, S., Asano, M., Horai, R., Sakaguchi, N. & Iwakura, Y. (2001) *J. Immunol.* **167**, 90–97.
19. Saijo, S., Asano, M., Horai, R., Yamamoto, H. & Iwakura, Y. (2002) *Arthritis Rheum.* **46**, 533–544.
20. Jaiswal, A. I., Dubey, C., Swain, S. L. & Croft, M. (1996) *Int. Immunol.* **8**, 275–285.
21. Mori, S., Sawai, T., Teshima, T. & Kyogoku, M. (1988) *J. Histochem. Cytochem.* **36**, 111–114.
22. Durie, F. H., Fava, R. A., Foy, T. M., Aruffo, A., Ledbetter, J. A. & Noelle, R. J. (1993) *Science* **261**, 1328–1330.
23. Webster, E. A., Khakoo, A. Y., Mackus, W. J., Karpusas, M., Thomas, D. W., Davidson, A., Christian, C. L. & Lederman, S. (1999) *Arthritis Rheum.* **42**, 1291–1296.
24. Yoshioka, T., Nakajima, A., Akiba, H., Ishiwata, T., Asano, G., Yoshino, S., Yagita, H. & Okumura, K. (2000) *Eur. J. Immunol.* **30**, 2815–2823.
25. Weinberg, A. D. (2002) *Trends Immunol.* **23**, 102–109.
26. Wagner, U. G., Kurtin, P. J., Wahner, A., Brackertz, M., Berry, D. J., Goronzy, J. J. & Weyand, C. M. (1998) *J. Immunol.* **161**, 6390–6397.
27. Yellin, M. J., Sippel, K., Inghirami, G., Covey, L. R., Lee, J. J., Sinning, J., Clark, E. A., Chess, L. & Lederman, S. (1994) *J. Immunol.* **152**, 598–608.
28. Higuchi, T., Aiba, Y., Nomura, T., Matsuda, J., Mochida, K., Suzuki, M., Kikutani, H., Honjo, T., Nishioka, K. & Tsubata, T. (2002) *J. Immunol.* **168**, 9–12.
29. Yao, Z., Fanslow, W. C., Seldin, M. F., Rousseau, A. M., Painter, S. L., Comeau, M. R., Cohen, J. I. & Spriggs, M. K. (1995) *Immunity* **3**, 811–821.

Journal of Neurochemistry, 2003, 85, 1412–1420 doi:10.1046/j.1471-4159.2003.01787.x

Interleukin-18 induces expression and release of cytokines from murine glial cells: interactions with interleukin-1β

Rachel D. Wheeler,* David Brough,* Rosalind A. Le Feuvre,* Kiyoshi Takeda,† Yoichiro Iwakura,‡ Giamal N. Luheshi§ and Nancy J. Rothwell*

*School of Biological Sciences, University of Manchester, Oxford Road, Manchester, UK
†Hyogo College of Medicine, Hyogo, Japan
‡Center for Experimental Medicine, Institute of Medical Science, University of Tokyo, Tokyo, Japan
§Douglas Hospital Research Center, McGill University, Verdun, Quebec, Canada

Abstract

Interleukin (IL)-18, a member of the IL-1 cytokine family, is an important mediator of peripheral inflammation and host defence responses. IL-1 is a key proinflammatory cytokine in the brain, but the role of IL-18 in the CNS is not yet clear. The objective of this study was to investigate the actions of IL-18 on mouse glial cells. IL-18 induced intracellular expression of IL-1α and proIL-1β, and release of IL-6 from mixed glia. Treatment of lipopolysaccharide-primed microglia with adenosine triphosphate (ATP), an endogenous secondary stimulus, induced IL-1β and IL-18 release. Although deletion of the IL-18 gene did not affect IL-1β expression or release in this experimental paradigm, IL-1β knockout microglia released significantly less IL-18 compared to wild-type microglia. In addition, ATP induced release of mature IL-1β from IL-18-primed microglia. These data suggest that IL-18 may contribute to inflammatory responses in the brain, and demonstrate that, in spite of several common features, IL-18 and IL-1β differ in their regulation and actions.

Keywords: ATP, caspase-1, glia, IL-18, IL-1β.
J. Neurochem. (2003) **85**, 1412–1420.

Interleukin (IL)-1 is a major proinflammatory cytokine that exerts many actions in the brain, such as induction of fever, enhancement of sleep and exacerbation of neurodegeneration (for review, see Allan and Rothwell 2001). IL-18, a member of the IL-1 cytokine family (Bazan *et al.* 1996), is a key mediator in peripheral inflammation and host defence responses (Nakanishi *et al.* 2001). IL-18 and IL-1 (which has two agonist forms, IL-1α and IL-1β) act through related receptor complexes, consisting of a ligand-binding chain (IL-18Rα or IL-1R, respectively) and an accessory chain (IL-18Rβ or IL-1R AcP, respectively), to trigger common signalling pathways (Fantuzzi and Dinarello 1999; Fitzgerald and O'Neill 2000).

IL-18, its receptor complex, and IL-18 binding protein (IL–18BP), an endogenous inhibitor of IL-18, are expressed constitutively in rat brain (Wheeler *et al.* 2000), but its role in the brain is not yet clear. IL-18 enhances non-rapid eye movement sleep in rabbits and rats, and neutralization of IL-18 in rabbits inhibits muramyl dipeptide-induced sleep (Kubota *et al.* 2001), suggesting that endogenous IL-18 has specific actions in the brain. Furthermore, intracerebroventricular injection of high doses of IL-18 elevates brain temperature but, unlike IL-1, peripheral administration of IL-18 is not pyrogenic (Kubota *et al.* 2001; Gatti *et al.* 2002). IL-18 mRNA is upregulated during the acute phase of experimental autoimmune encephalomyelitis or neuritis in rats, in the brain and nerve roots, respectively (Jander and Stoll 1998, 2001). IL-18 levels are elevated in the cerebrospinal fluid of patients with bacterial meningitis (Fassbender *et al.* 1999) and IL-18 is upregulated in the late stages of focal cerebral ischaemia, and in neonatal

Received November 25, 2002; revised manuscript received February 5, 2003; accepted February 27, 2003.

Address correspondence and reprint requests to Rachel D. Wheeler, Neuroimmunology, Montreal Neurological Institute, 3801 University Street, Montreal, QC, Canada H3A 2B4.
E-mail: rachel.wheeler@mail.mcgill.ca

Abbreviations used: ATP, adenosine triphosphate; DIV, days *in vitro*; DMEM, Dulbecco's modified Eagle's medium; DTT, dithiothreitol; ELISA, enzyme-linked immunosorbent assays; HRP, horseradish peroxidase; IL-18BP, interleukin-18 binding protein; IL-18R, interleukin-18 receptor; LDH, lactate dehydrogenase; LPS, lipopolysaccharide; MMLV, myeloleukaemia virus reverse transcriptase; PBS, phosphate-buffered saline; SDS–PAGE, sodium dodecyl sulphate polyacrylamide gel electrophoresis.

